

Modeling potential masking of echolocating sperm whales exposed to continuous 1–2 kHz naval sonar

A. M. von Benda-Beckmann, S. Isojunno, M. Zandvliet, et al.

Citation: *The Journal of the Acoustical Society of America* **149**, 2908 (2021); doi: 10.1121/10.0004769

View online: <https://doi.org/10.1121/10.0004769>

View Table of Contents: <https://asa.scitation.org/toc/jas/149/4>

Published by the [Acoustical Society of America](#)

ARTICLES YOU MAY BE INTERESTED IN

[Echolocation click parameters of short-finned pilot whales \(*Globicephala macrorhynchus*\) in the wild](#)
The Journal of the Acoustical Society of America **149**, 1923 (2021); <https://doi.org/10.1121/10.0003762>

[Near real-time detection of low-frequency baleen whale calls from an autonomous surface vehicle: Implementation, evaluation, and remaining challenges](#)
The Journal of the Acoustical Society of America **149**, 2950 (2021); <https://doi.org/10.1121/10.0004817>

[Acoustic detection range and population density of Cuvier's beaked whales estimated from near-surface hydrophones](#)
The Journal of the Acoustical Society of America **149**, 111 (2021); <https://doi.org/10.1121/10.0002881>

[Separating overlapping echolocation: An updated method for estimating the number of echolocating animals in high background noise levels](#)
The Journal of the Acoustical Society of America **150**, 709 (2021); <https://doi.org/10.1121/10.0005756>

[Multi-sensor integration for an assessment of underwater radiated noise from common vessels in San Francisco Bay](#)
The Journal of the Acoustical Society of America **149**, 2451 (2021); <https://doi.org/10.1121/10.0003963>

[Techniques for distinguishing between impulsive and non-impulsive sound in the context of regulating sound exposure for marine mammals](#)
The Journal of the Acoustical Society of America **147**, 2159 (2020); <https://doi.org/10.1121/10.0000971>

JASA
THE JOURNAL OF THE
ACOUSTICAL SOCIETY OF AMERICA

**Special Issue: Fish Bioacoustics:
Hearing and Sound Communication**

CALL FOR PAPERS

Modeling potential masking of echolocating sperm whales exposed to continuous 1–2 kHz naval sonar

A. M. von Benda-Beckmann,^{1,a)} S. Isojunno,² M. Zandvliet,¹ M. A. Ainslie,^{3,b)} P. J. Wensveen,⁴ P. L. Tyack,² P. H. Kvadsheim,⁵ F. P. A. Lam,¹ and P. J. O. Miller²

¹Acoustics and Sonar, Netherlands Organization for Applied Scientific Research (TNO), P.O. Box 96864, The Hague 2509 JG, The Netherlands

²Sea Mammal Research Unit, Scottish Oceans Institute, School of Biology, University of St Andrews, St Andrews, Fife KY16 8LB, United Kingdom

³JASCO Applied Sciences (Deutschland) GmbH, Eschborn, Germany

⁴Faculty of Life and Environmental Sciences, University of Iceland, Askja, Sturlugata 7, 102 Reykjavik, Iceland

⁵Sensor and Surveillance Systems, Norwegian Defense Research Establishment (FFI), NO-3191 Horten, Norway

ABSTRACT:

Modern active sonar systems can (almost) continuously transmit and receive sound, which can lead to more masking of important sounds for marine mammals than conventional pulsed sonar systems transmitting at a much lower duty cycle. This study investigated the potential of 1–2 kHz active sonar to mask echolocation-based foraging of sperm whales by modeling their echolocation detection process. Continuous masking for an echolocating sperm whale facing a sonar was predicted for sonar sound pressure levels of 160 dB re 1 μPa^2 , with intermittent masking at levels of 120 dB re 1 μPa^2 , but model predictions strongly depended on the animal orientation, harmonic content of the sonar, click source level, and target strength of the prey. The masking model predicted lower masking potential of buzz clicks compared to regular clicks, even though the energy source level is much lower. For buzz clicks, the lower source level is compensated for by the reduced two-way propagation loss to nearby prey during buzzes. These results help to predict what types of behavioral changes could indicate masking in the wild. Several key knowledge gaps related to masking potential of sonar in echolocating odontocetes were identified that require further investigation to assess the significance of masking. © 2021 Acoustical Society of America. <https://doi.org/10.1121/10.0004769>

(Received 14 October 2020; revised 1 April 2021; accepted 2 April 2021; published online 30 April 2021)

[Editor: Brian Branstetter]

Pages: 2908–2925

I. INTRODUCTION

The introduction of new high-power sources of (almost) continuous sound into the underwater environment by humans raises questions about their effects on marine life. Conventional pulsed active sonars (PASs) used in anti-submarine warfare transmit intermittently, and their effects on marine mammal behavior have been studied in the last two decades (Miller *et al.*, 2012; Harris *et al.*, 2018; Southall *et al.*, 2019). New sonars that continuously transmit sound and simultaneously receive faint echoes, a technology called continuous active sonar (CAS), are enabled by increased source bandwidth, receiver dynamic range, and increased processing power of modern acoustic receivers (Van Vossen *et al.*, 2011; Bates *et al.*, 2018; Hines *et al.*, 2015). A similar technological trend is also seen within seismic surveys where marine vibrators or conventional airguns are used to create low frequency signals with increased transmission time (Oscarsson-Nagel *et al.*, 2019; Hegna *et al.*, 2018). The increased transmission time and duty cycle of CAS may lead to different responses by animals and may particularly

increase the masking potential compared to PAS because CAS provides fewer opportunities to listen between pulses (“dip listening”; Sills *et al.*, 2017).

The masking potential of low frequency (<1 kHz) continuous noise sources, such as natural wind-generated noise, shipping noise, and continuous distant airgun sounds, has received some attention (Clark *et al.*, 2009; Guan *et al.*, 2015; Erbe *et al.*, 2016; Aulancier *et al.*, 2017; Dunlop, 2018). However, though one study carried out in 2016 and 2017 investigated behavioral changes of sperm whales in Norwegian waters in response to continuous active sonar exposures (Isojunno *et al.*, 2020), the masking potential of high-power continuous sonar sources operating at the higher frequencies used in some naval sonars has not yet been considered.

Active sonar used in anti-submarine warfare typically transmits pulses in the range of 1–10 kHz (D’Amico and Pittenger, 2009). These sonar frequencies are lower than what is believed to be the main echolocation band of sperm whales (Møhl *et al.*, 2003), but sperm whale clicks do contain energy at these lower frequencies and broader beam patterns that may propagate out to larger distances. Active sonar transmissions may also contain significant harmonic content at higher frequencies [Fig. 1; see also Guan *et al.* (2017)], which contributes to the masking potential.

^{a)}Electronic mail: sander.vonbendabeckmann@tno.nl, ORCID: 0000-0002-4210-8058.

^{b)}ORCID: 0000-0002-0565-3559.

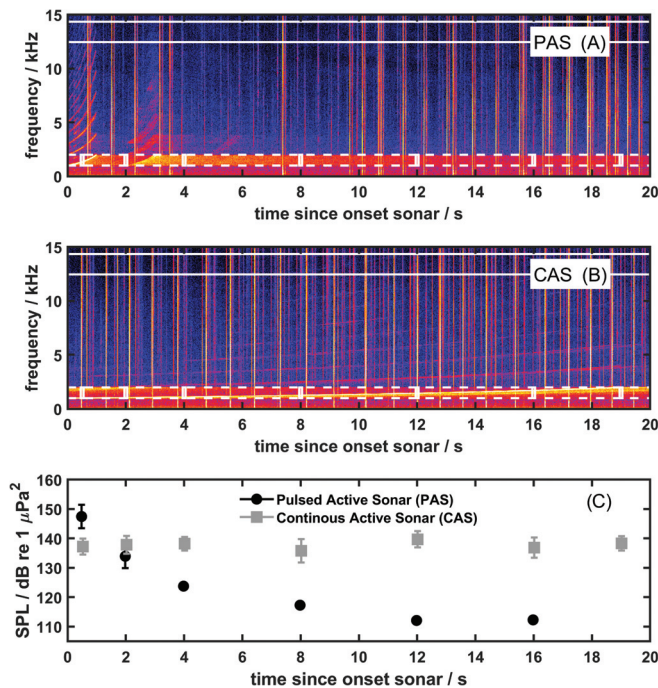


FIG. 1. Example of DTAG recordings of PAS (A) and CAS (B) on a tagged sperm whale exposed to sonar sounds (Isojunno *et al.*, 2020). The white lines delimit the main sperm whale echolocation effective detection bandwidth (solid lines at 12.5 and 14.5 kHz) and the 1–2 kHz sonar transmission band (dashed lines). Vertical lines in the spectrograms are sperm whale echolocation clicks produced by the tagged individual and other nearby animals simultaneously recorded by the DTAG. (C) Received SPL measured over the frequency band of 1–2 kHz and within a 0.1 s time window at varying delays since the onset of the sonar pulse [marked as white boxes in (A) and (B)]. Mean [and standard deviation (SD)] SPLs were determined over 45 transmissions with the source transmitting at SL = 214 dB re 1 μPa²·m² for PAS and SL = 201 dB re 1 μPa²·m² for CAS and a 20 s repetition time (Isojunno *et al.*, 2020). Average SPLs clearly show the decaying SPL with time for the PAS signal due to reverberation after the signal ends, whereas the SPL remains constant throughout the CAS signal transmission.

Male sperm whales are found in high-latitude feeding areas, while females and juveniles are thought to remain in lower latitudes (Whitehead, 2003). During foraging dives, sperm whales produce regular (“usual”) echolocation clicks with inter-click intervals (ICIs; the reciprocal of the click repetition rate) ranging typically between 0.4 and 1.2 s; this is considered the searching phase (Miller *et al.*, 2004; Teloni *et al.*, 2008; Tønnesen *et al.*, 2020). When animals approach their prey, they switch to a sequence of clicks, called a “buzz,” with much shorter ICIs between 0.01 and 0.1 s, which likely provides faster updates that allow them to catch moving prey (Gordon, 1987; Madsen *et al.*, 2002; Miller *et al.*, 2004). Sperm whales sometimes forage close to the seafloor, but they typically target prey in the water column (Teloni *et al.*, 2008). Buzz duration and periods between buzzes depend strongly on the foraging depth, which is likely driven by differences in prey type that these animals feed on at different depths and ambient pressure (Teloni *et al.*, 2008; Isojunno and Miller, 2018). Differences in buzz duration, timing between buzzes, and movement behavior during shallow and deep dives suggest that different prey types are targeted. Sperm whales tend to use shorter

buzzes when foraging at depth, where they are thought to target less mobile cephalopods. Longer buzzes recorded near the surface are associated with more maneuvering and longer periods between buzzes, suggesting a hunt for mobile prey, such as large fish or muscular cephalopods (Teloni *et al.*, 2008; Fais *et al.*, 2016; Isojunno and Miller, 2018). This varied diet is also supported by analyses of stomach contents in sperm whales (Rice, 1989; Santos *et al.*, 1999).

The objective of this study was to identify scenarios (geometry relative to masker, prey type/distance, click types) in which the masking potential for sperm whales is high. A theoretical assessment was carried out to understand the masking potential of 1–2 kHz naval sonar on the echolocation of sperm whales and whether some of the previously reported changes in foraging behavior in response to this type of sonar (Miller *et al.*, 2012; Sivle *et al.*, 2015; Isojunno *et al.*, 2016; Isojunno *et al.*, 2020) could be due to masking. This can support the interpretation of empirical analyses of changes in sperm whales’ echolocation behavior in relation to sonar exposures (Isojunno *et al.*, 2020).

Masking can be defined in different ways but in general occurs when the perception of an acoustic stimulus is degraded by other acoustic (masker) stimuli (Durlach, 2006; Slabbekoorn *et al.*, 2018). A large body of literature exists on masking in humans and other terrestrial species (Slabbekoorn *et al.*, 2018), but much less is understood about masking in marine mammals, which have adapted to use underwater sound as one of their primary sensory capabilities for foraging, orientation, and communication (Erbe *et al.*, 2016). Many animals have evolved different mechanisms to cope with masking sounds. These mechanisms involve auditory processes, such as dip-listening (Wiley and Richards, 1982; Klump, 1996), co-modulating masking release (Moore, 2003; Branstetter *et al.*, 2013), auditory stream segregation (Bregman, 1990; Vliegen and Oxenham, 1999), spatial masking release (Arbogast *et al.*, 2002; Saberi *et al.*, 1991; Hine *et al.*, 1994; Dent *et al.*, 1997; Sümer *et al.*, 2009), or use of multi-modal signal integration with other (e.g., visual) cues (Brumm and Slabbekoorn, 2005). Adaptations of acoustic behavior to avoid masking can also be active, for instance, by increasing source levels of sounds (Lane and Tranel, 1971), changing the frequency spectrum (Halfwerk and Slabbekoorn, 2009; Gross *et al.*, 2010; Verzijden *et al.*, 2010), or temporally adapting signals to avoid overlap with noise (Fuller *et al.*, 2007; Planque and Slabbekoorn, 2008).

Characteristics of sperm whale echolocation signals have been studied through passive acoustic monitoring. These studies show that sperm whale clicks are emitted at high on-axis source levels and have a high directionality and relatively low peak and centroid frequencies compared to other echolocation odontocetes, which have likely evolved to allow for long-distance detection of prey during deep dives (Møhl *et al.*, 2003; Madsen *et al.*, 2002; Madsen *et al.*, 2007; André *et al.*, 2007; Au and Hastings, 2008; Jensen *et al.*, 2018, Tønnesen *et al.*, 2020). Data on the hearing capabilities of adult sperm whales are not available

(Ridgway and Carder, 2001; Erbe *et al.*, 2016; Southall *et al.*, 2019). Evaluation of masking potential in sperm whales in the wild therefore requires extrapolation from what is known from captive studies of other species. The effect of masking on marine mammal hearing has only been studied in a limited number of species in captivity: dolphins, belugas, porpoises, false-killer whales, and killer whales (Au and Moore, 1984; Au, 2014; Kastelein *et al.*, 2005; Erbe, 2008; Bain and Dahlheim, 1994; Branstetter *et al.*, 2013; Popov *et al.*, 2020).

This literature was reviewed to construct a masking model for echolocating sperm whales, which was used to explore the potential for masking under different natural ambient sound conditions and conditions in which sperm whales may be exposed to continuous and pulsed active sonar. Further, some of the key knowledge gaps related to masking potential of sonar in echolocating marine mammals are highlighted.

II. METHODS

A. Modeling masking of echolocation clicks in sperm whales

Auditory masking is notoriously difficult to quantify accurately in animals in the wild, since the information contained in the signals is often unknown, animals may not respond to biologically meaningful signals that are audible, and the hearing capabilities of many species, especially large marine mammals, are not well understood. Energetic masking is often used as the basis for modeling masking in echolocating species (Au, 1993; Au *et al.*, 2004; Au, 2014; Madsen *et al.*, 2002; Madsen *et al.*, 2007; Ainslie, 2010; Erbe *et al.*, 2016; Dooling and Leek, 2018).

The echolocation performance of sperm whales under masked conditions was modeled as an energy detection process within an effective detection bandwidth B_{eff} and hearing integration time of the echolocation click t_{int} , based on observations from trained captive bottlenose dolphins carrying out target detection echolocation tasks (Au and Moore, 1984; Au, 2014). To model the energy detector, the energy version for the active sonar equation in the form presented in Ainslie (2010) was considered: It expresses the level of the signal-to-noise ratio (SNR) as a function of echo energy level (EL_E), background energy level (BL_E ; including the ambient and masker sounds), and processing gain (PG; the amount of spatial masking release),

$$\text{SNR} = EL_E - (BL_E - \text{PG}). \quad (1)$$

Except where otherwise stated, we follow the notation and definitions of Ainslie (2010). In Eq. (1), the EL_E depends on click energy source level (ESL), two-way propagation loss (outgoing PL_T and return PL_R), and target strength (TS) of the prey,

$$EL_E = \text{ESL} - (PL_T + PL_R) + \text{TS}. \quad (2)$$

Note that the SNR for sperm whales likely depends on the target bearing and elevation from the whale, since both the

transmitted echolocation click and hearing are highly directional. The on-axis SNR for a target prey directly in front of the animal was considered (Fig. 2). Calculations of the two-way propagation loss assumed spherical spreading and frequency-dependent absorption (Ainslie, 2013; von Benda-Beckmann *et al.*, 2018).

Two types of sperm whale echolocation clicks were considered: regular echolocation clicks used during the search phase and buzz clicks used during prey capture attempts (Miller *et al.*, 2004). The regular clicks represent on-axis echolocation clicks (Møhl *et al.*, 2003), which have a centroid frequency of $f_c = 13.4\text{--}15$ kHz, peak frequencies around 12 kHz, and a root mean square (rms) bandwidth (Au and Hastings, 2008) $B_{\text{rms}} = 4.1$ kHz (Møhl *et al.*, 2003; Jensen *et al.*, 2018). The regular click source level (rms over 52 μs) was found to range between 220 and 236 dB re 1 $\mu\text{Pa}^2 \cdot \text{m}^2$, with a corresponding ESL = 187–198 dB re 1 $\mu\text{Pa}^2 \cdot \text{m}^2 \cdot \text{s}$ (Madsen *et al.*, 2002; Møhl *et al.*, 2003). Buzz clicks contain a similar or slightly larger f_c and B as regular echolocation clicks but are transmitted at approximately 26–53 dB lower ESL compared to echolocation clicks, with a range of ESLs measured at different angles from the sperm whale axis of ESL = 145–161 dB re 1 $\mu\text{Pa}^2 \cdot \text{m}^2 \cdot \text{s}$ (Madsen *et al.*, 2002; Fais *et al.*, 2016). For practical purposes, the same click waveform for both regular and buzz clicks was adopted in the masking model.

B. Masking criterion

The SNR was estimated within an effective detection bandwidth around the peak frequency of sperm whale echolocation clicks using Eq. (1). The detection threshold (DT) for detecting a target under masked conditions has been measured in captive bottlenose dolphins (Au, 2014). Since data are lacking on the hearing system of sperm whales, it was assumed that the ratio $Q_{\text{eff}} = f_p / B_{\text{eff}}$, of the effective detection bandwidth, B_{eff} , and the peak frequency, as well as the hearing integration time, t_{int} , are similar to those of bottlenose dolphins (Au, 2014) but shifted to the observed centroid frequency of on-axis sperm whale clicks (Møhl *et al.*, 2003; Madsen *et al.*, 2002). In addition, it was assumed that within this bandwidth and integration time, the detection threshold of a sperm whale is similar to that of a bottlenose dolphin.

Au (2014) found that a detection probability of 50% under masked conditions (DT50), measured within the effective detection bandwidth and the hearing integration time for echolocation clicks, was achieved at a SNR close to zero (1 dB) and that a 95% detection probability was achieved at a mean SNR (DT95) of 6 dB (range 3–11 dB). Since the objective here was to identify scenarios where echoes were likely to be masked, a 6 dB detection threshold was adopted as a threshold for determining the detection distance.

The peak frequency of clicks by a bottlenose dolphin (*Tursiops truncatus*; abbreviated as *tt*) carrying out an echolocation task was 120 kHz. The -3 dB hearing filter

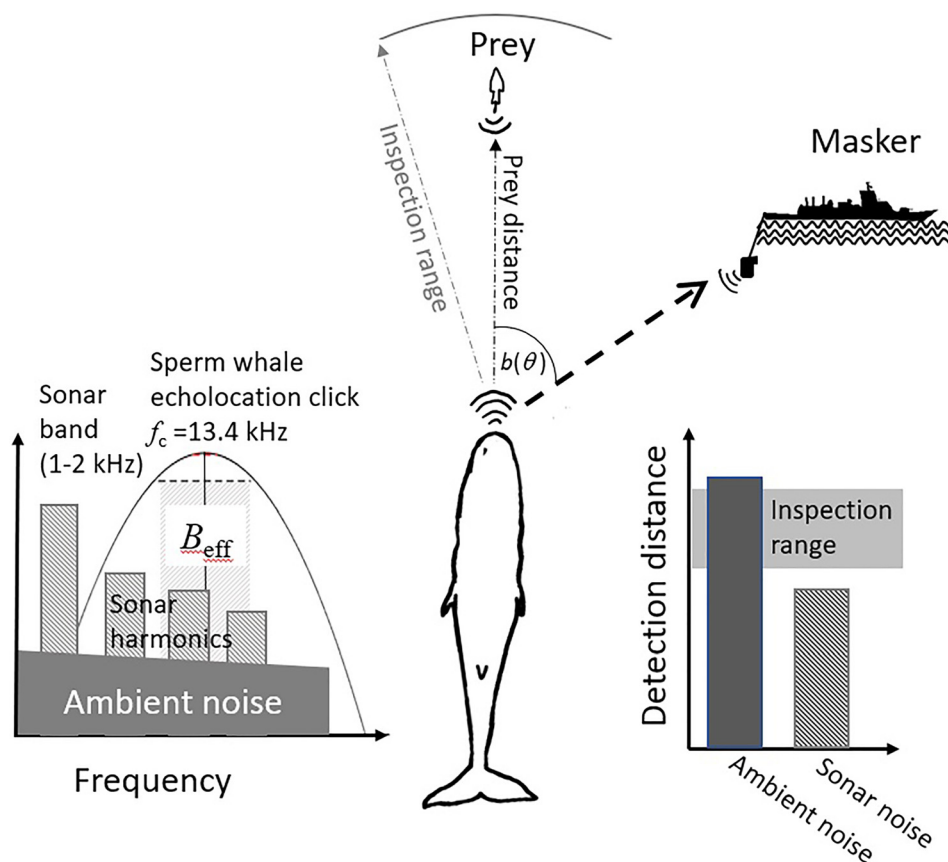


FIG. 2. (Color online) Schematic of the sperm whale echolocation masker model used for evaluating the potential for masking by low frequency sonar (LFAS) of faint echoes from prey. Left inset: The dominant part of LFAS is at frequencies 1–2 kHz, outside the sperm whale effective detection band (B_{eff}) centered around $f_c = 13.4$ kHz, but sonar harmonics may contribute to the masking potential. Echolocation occurs under ambient conditions, typically masked by wind-generated noise from the sea surface and from reverberation of the echolocation click echoes. Middle inset: The amount of spatial masking release $b(\theta)$ experienced by the sperm whale depends on the angle θ of the masking sound source relative to the prey in front of the animal. Right inset: Masking is considered likely to occur when the masked detection distance falls below the inspection range (determined by the ICI) used by sperm whales during baseline foraging.

bandwidth around this peak frequency was independently measured to be 16.7 kHz for this individual; hence, $Q_{\text{eff}} = f_{p, \text{eff}} / B_{\text{eff}, \text{eff}} = 7.1$ (Lemonds *et al.*, 2012; Au, 2014), somewhat narrower than 1/3-octave band often assumed for masked detection but in the range of critical bandwidths observed in odontocetes for tonal sounds (Erbe *et al.*, 2016). This effective detection bandwidth was used by Au (2014) to derive detection thresholds for dolphins. The integration time for click detection for dolphins has been estimated at 264 μs (Au *et al.*, 1988). Since the centroid frequency of sperm whale clicks is 13.4 kHz, an effective bandwidth of $B_{\text{eff}} = f_c / Q_{\text{eff}} = 1.9$ kHz was adopted. Centroid frequency was used because it is a more stable quantity for broadband signals than peak frequency, and the centroid frequency and peak frequency of dolphin clicks studied in Au (2014) were similar (within a few kHz; Au and Hastings, 2008). Based on the click spectra presented in Madsen *et al.* (2002), the sperm whale click energy within this effective detection band could not be measured directly. A correction factor was estimated by approximating the click with a Gabor wavelet with the same centroid frequency and -3 dB bandwidth (see the Appendix). The difference between the total click energy and energy within the effective detection band was used to correct the click ESL as follows: $\text{ESL}_{Q_{\text{eff}}} = \text{ESL} - 5$ dB. Detection distances R_d corresponding to the distance at which the $\text{SNR} = \text{SNR}_{95\%}$ were computed.

Sperm whales were assumed to actively detect prey within a maximum distance related to the two-way travel time (TWTT) determined by the ICI (i.e., the inspection

range = $\text{TWTT} / 2 \cdot c_s$; Jensen *et al.*, 2018). Echolocating odontocetes often adjust their ICI to a little more than the TWTT to a known target (Au *et al.*, 1974; Thomas and Turl, 1990; Madsen *et al.*, 2005; Verfuß *et al.*, 2005; Wisniewska *et al.*, 2015; Ladegaard *et al.*, 2017), although deep-diving beaked whales, sperm whales, and dolphins may use ICIs much longer than the TWTT to the prey they are about to capture (Madsen *et al.*, 2005; Jensen *et al.*, 2018; Tønnesen *et al.*, 2020).

To assess whether the detection of echoes was significantly masked, the typical inspection range was based on observed ICIs of sperm whales feeding in high-latitude environments (Teloni *et al.*, 2008; Fais *et al.*, 2015; Isojunno and Miller, 2018). ICIs following prey capture attempts may correspond more closely to the distances at which the animal is looking for prey and are typically somewhat shorter than used at the start of a dive (Fais *et al.*, 2015). For regular clicks, the inspection range was based on the typical distribution of observed ICIs after prey capture attempts, which ranged between 0.2 and 1 s (Fais *et al.*, 2015), from which we considered the mean ICI of 0.6 s to determine the relevant inspection range during the regular clicking phase. A recent study indicates that sperm whales switch from regular clicks to buzzes when prey distances are approximately 1–2 times the body size (Fais *et al.*, 2016; Tønnesen *et al.*, 2020). This is a somewhat larger distance than is observed for smaller odontocetes (Madsen and Surlykke, 2013) and may be caused by the limited maneuverability of sperm whales (Fais *et al.*, 2016; Tønnesen *et al.*, 2020). For buzzes,

we therefore adopted a relevant inspection range for the buzz phase of $2 \times$ (average body size) of an adult male sperm whale, which is approximately 26 m. Masking was assumed to occur when R_d was smaller than the relevant inspection range during the regular and buzz phase. Minimum and maximum ICI observed during regular clicking (Fais *et al.*, 2015) and during the buzz phase (Isojunno and Miller, 2018) were used to indicate the range of relevant inspection ranges.

1. Masking noise: Ambient noise

The range of echolocation in natural conditions is often limited by wind- and rain-generated ambient noise. These are the dominant noise source in the frequencies around 13 kHz (Wenz, 1962; Madsen *et al.*, 2002) relevant to sperm whale echolocation unless the animal is echolocating close to the seafloor or surface, where it could be reverberation limited by its own biosonar. Several different noise conditions were considered, expressed in terms of the sea state (SS). Noise levels were estimated using Wenz curves for three different SSs: 1, 2, and 4. The noise field in deep water is highly directional from the surface, with relatively little contribution of high-frequency sound from the direction of the sea floor (Cron and Sherman, 1962; Short, 2005; Barclay and Buckingham, 2013). Hence, a sperm whale foraging in a pelagic prey field, directed away from the sea surface, is likely to benefit from a strong reduction of the interfering ambient noise because of spatial masking release due to its directional hearing.

2. Masking noise: Sonar exposure test data

Controlled sonar experiments with a 1–2 kHz sonar source were used to compare the behavioral responses of sperm whales to PAS and CAS during phase III of the Sea Mammals, Sonar, Safety (3S3) behavioral response study (Isojunno *et al.*, 2020). During these experiments, a sperm whale equipped with a digital recording tag (DTAG) was approached by a vessel towing a sonar source (Socrates; Miller *et al.*, 2012) that transmitted PAS or CAS hyperbolic-frequency modulated (HFM) upsweeps (Ainslie, 2010) of 1 and 19 s duration, respectively, with a pulse repetition time of 20 s (Fig. 1). In addition to the controlled approach of the animal by the source, the experimental dose-escalation design included a ramp up of the source level (Isojunno *et al.*, 2020). This design led to typical received sound pressure levels (SPLs) in the 1–2 kHz band, $L_{p,1-2\text{kHz}}$, from 120 up to 180 dB re $1 \mu\text{Pa}^2$ for PAS and up to 160 dB re $1 \mu\text{Pa}^2$ for CAS. This range of received levels was considered in this study to assess the masking potential.

The harmonic energy content for frequencies exceeding the sonar design frequencies is rarely quantified and could not be reliably measured on the DTAG due to the system noise floor. To obtain realistic SPLs in the echolocation band of the sperm whale a (range of) level difference ΔL_{hrmc} of the sonar harmonics signal in the echolocation band relative to the 1–2 kHz sonar band was estimated using two

separate datasets:¹ a dedicated experiment measuring harmonics, where the Socrates source transmitted at a fixed distance (approximately 1 km) from a recorder deployed from a rigid-hulled inflatable boat (RHIB) using continuous wave (CW) transmissions at different source levels (SLs) at different depths (Lam *et al.*, 2018), and a second dataset based on bottom-moored broadband acoustic recorders during the controlled exposure experiments of Isojunno *et al.* (2020), at distances varying from 500 to 10 000 m from the source.

These analyses showed that the harmonic content of the sonar signal in the sperm whale echolocation band varied strongly over time, even for a constant SL and SPL at the fundamental frequency.¹ Typically, 1–3 harmonics were observed within the effective detection band of sperm whales. The harmonic levels, when corrected for the difference in frequency-dependent attenuation to account for variability in sonar-to-recorder distance in the dataset, were found to lie between $\Delta L_{\text{hrmc}} = -80$ and -38 dB relative to the SPL in the 1–2 kHz band. The variation could have had several causes: frequency-dependent harmonic level, horizontal and vertical directionality of the sound at higher frequencies, source depth, receiver depth, and differences in propagation conditions that affected higher frequencies differently than lower frequencies.

The sonar noise levels in the sperm whale effective detection band were estimated by subtracting a constant factor ΔL_{hrmc} from the level in the 1–2 kHz band ($L_{p,13.4\text{kHz}} = L_{p,1-2\text{kHz}} - \Delta L_{\text{hrmc}}$), where a range of sonar levels $L_{p,1-2\text{kHz}} = 120, 140, \text{ and } 160$ dB re $1 \mu\text{Pa}^2$ and harmonic content factors $\Delta L_{\text{hrmc}} = -38, -59, \text{ and } -80$ dB were considered. An ambient noise level corresponding to a SS = 2 (typical condition during the 3S3 experiments) was adopted in cases where the harmonic levels were below ambient noise.

C. Spatial masking release

The PG in an animal's biosonar system is influenced partly by the amount of spatial masking release that may occur when the masking source is located at a different angle than the prey that the sperm whale is targeting. Spatial masking release can be quantified as the difference in masked hearing thresholds of the situation where the signal and masker are coming from two directions and the situation where the signal and masking sound are coming from the same direction. In this study, we considered prey echoes (the signal) coming from in front of the animal ($\theta = 0^\circ$). To estimate the amount of spatial masking release in sperm whales, two cases were considered: an animal facing the masker (PGmin = 0 dB) and an animal facing 90° away from the masker benefiting from a spatial masking release (PGmax). Spatial masking studies and directional hearing studies indicated an increase in hearing thresholds and similar degree of masking release with increased source angle θ up to 180° (Popov *et al.*, 2020). The amount of spatial masking release (commonly expressed in terms of the directivity index (DI) for an omnidirectional masker) depends on the

TABLE I. Estimated centroid frequencies (f_c), peak frequency (f_p), bandwidth (B_{rms}), and head size (a_{head}) for the five species used in estimating the amount of spatial masking release in sperm whales. Click frequencies and bandwidths were taken from Jensen *et al.* (2018), and head size estimates were taken from Shaffer *et al.* (2013).

	f_c (kHz)	f_p (kHz)	B_{rms} (kHz)	a_{head} (cm)
Harbor porpoises (<i>Phocoena phocoena</i>)	137	138	10	14.8
Bottlenose dolphins (<i>Tursiops truncatus</i>)	77	120	32	28.6
Beluga whale (<i>Delphinapterus leucas</i>)	41	—	13	39.8
Killer whale (<i>Orcinus orca</i>)	37	29	12	92.95 ^a
Sperm whale (<i>Physeter macrocephalus</i>)	15	15	4.1	240 ^b

^aThe ratio of head size between killer whale and a bottlenose dolphin, a_{OO}/a_{TT} , varies between 3 and 3.5 (Au *et al.*, 2004). Here, a ratio of 3.25 was chosen.
^bHead size estimated as 15% of body length (Nishiwaki *et al.*, 1963) with a typical body length of adult male sperm whale of 16 m (Whitehead, 2018).

frequency as well as the size of the animal (Au and Moore, 1984; Kastelein *et al.*, 2005). The DI quantifies the gain of a directional receiver exposed to an omnidirectional masker and plane wave signal. Diving sperm whales echolocating for prey often face away from the sea surface and from the sonar source; hence, the amount of masking release for an animal facing away from the sonar (i.e., at $\theta = 90^\circ$) is more representative for modeling the masking potential of ambient and sonar sound in diving sperm whales than using reported DI values.

A comparative study on the directionality of the echolocation click beam pattern showed that the (transmitted) DI is relatively constant over a large range of species and body masses and corresponding center frequencies (Jensen *et al.*, 2018). It has been argued that hearing directionality may show a similar scaling with frequency and head size (Au *et al.*, 2004). To estimate the amount of spatial masking release in sperm whales for a masking source at 90° from the animal, $b(90)$, two types of measurements were combined to achieve a wide range of odontocete body sizes: (1) masked thresholds with a noise source positioned at 90° measured for other cetacean species; (2) the difference in hearing threshold for measurements with the source projecting toward the most sensitive forward ($\theta = 0^\circ$) body orientation vs projecting at 90° angles. These were available for four different odontocete species spanning a large range in body size and mass: harbor porpoises (Kastelein *et al.*, 2005), bottlenose dolphin (Au and Moore, 1984; Popov and Supin, 2009), beluga whale (Mooney *et al.*, 2008; Popov and Supin, 2009), and killer whales (Bain and Dahlheim, 1994). Masking release was available for harbor porpoise (Kastelein *et al.*, 2005), bottlenose dolphin (Au and Moore, 1984; Popov *et al.*, 2020), and killer whale (Bain and Dahlheim, 1994), and measured directional hearing threshold was available for beluga (Mooney *et al.*, 2008; Popov and Supin, 2009) and bottlenose dolphins (Popov and Supin, 2009; Accomando *et al.*, 2020). The relationships between the hearing directionality, centroid frequency, and head size were investigated to support the extrapolation of the masking release to sperm whales (Table I).

The amount of masking release as well as the relative hearing sensitivity measured at a 90° angle, $b(90)$, depended on frequency, body size, and centroid frequency used by four different odontocetes: harbor porpoises, bottlenose

dolphins, belugas, and killer whales (Fig. 3). Larger animals echolocate at lower frequencies (Jensen *et al.*, 2018) and also tend to achieve a higher masking release at lower frequencies. When the wavelength, λ , was scaled by head size, a_{head} , masking release shows a rough scaling with increasing a_{head}/λ , reaching levels of $b(90) = 13\text{--}24\text{ dB}$ for $a_{head}/\lambda > 10$

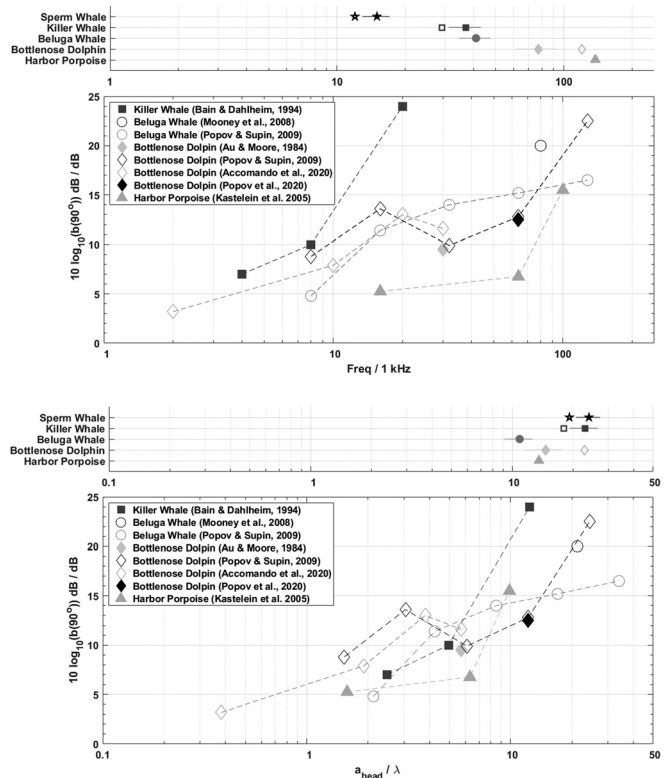


FIG. 3. Top panels: Echolocation click frequency. Symbols indicate centroid frequencies (filled), peak frequency (open), and rms bandwidth (solid horizontal line) for the echolocation clicks used by these different species in comparison to the sperm whale echolocation clicks from Jensen *et al.* (2018). Second panel: Off-axis masking release when the animal is facing 90° horizontally away from the masker ($\theta = 90^\circ$). Filled symbols are based on masking studies for different odontocete species: harbor porpoise (Kastelein *et al.*, 2005); bottlenose dolphin (Au and Moore, 1984; Popov *et al.*, 2020); killer whale (Bain and Dahlheim, 1994). Open symbols indicate the measured hearing threshold elevation relative to forward ($\theta = 0^\circ$) direction for a source projecting at 90° angle for two species: beluga (Popov and Supin, 2009; Mooney *et al.*, 2008) and bottlenose dolphins (Popov and Supin, 2009; Accomando *et al.*, 2020). Bottom panels: Same data shown in wavelengths and scaled by head size a_{head} . Values for the click parameters and head size a_{head} are provided in Table I.

TABLE II. Overview of model parameters used to model sperm whale masking potential. Sea state (SS)=2 conditions were assumed for the active sonar scenarios (indicated in boldface).

Spatial masking release	Click ESL (dB re 1 $\mu\text{Pa}^2\cdot\text{m}^2\cdot\text{s}$)				DT (dB) (detection probability)	Ambient sound (dB re 1 μPa^2)	Masker type	
	Regular click	Buzz click	Prey TS (dB re 1 m^2)	Sonar				
				$L_{p,1-2\text{kHz}}$ (dB re 1 μPa^2)			L_{hrmc} (dB)	
Facing toward masker (PG = 0 dB)	196 (high click ESL) 187 (low click ESL)	161	-40	1 (50%), 6 (95%)	65 (SS = 1), 70 (SS = 2) , 80 (SS = 4)	120, 140, 160	-80, -59, -38	
Facing 90° away from masker (PG = 20 dB)	196 (high click ESL) 187 (low click ESL)	145	-60	1 (50%), 6 (95%)	65 (SS = 1), 70 (SS = 2) , 80 (SS = 4)	120, 140, 160	-80, -59, -38	

for a wide range of body sizes. When we compared the centroid wavelengths (corresponding to the centroid frequency) of clicks of these species (Jensen *et al.*, 2018), the scaled centroid wavelength for all species exceeds $10 \cdot a_{\text{head}}/\lambda$. Although spatial masking release has not been measured in sperm whales, based on this scaling relationship of masking release with head size for different odontocete species and measured sperm whale click centroid wavelength, a maximum masking release of approximately 20 dB for sperm whales was determined as a plausible assumption. This was used in the remainder of this study to evaluate the effect of masking release on the masking potential of ambient and sonar sound when the animal was facing away from the masker.

D. Target strength of sperm whale prey

We considered a range of TSs (in units dB re 1 re m^2) appropriate for squid and large fish species. Typical squid length at depths targeted by sperm whales is $L \sim 25$ cm (André *et al.*, 2007). Different measurements of TS for squids have been reported. Møhl *et al.* (2003) estimated a TS of -40 dB based on Smith (1954). Based on TS measurements of different squid types made by Benoit-Bird *et al.* (2008), Ainslie (2010) derived an average relation for frequency in the range of 70–200 kHz of TS - $10\log_{10}(L^2/1 \text{ m}^2)$ dB = -27.6 dB. This corresponds to -40 dB using the typical squid size stated in André *et al.* (2007). Measurements by Benoit-Bird *et al.* (2008) indicated that TS of squid measured at different aspects varied by a maximum amount of 6 dB. More recently, André *et al.* (2007) measured that for a squid of length 25 cm, a TS = -36 ± 2.5 dB for frequencies of 15 kHz (around the peak frequency of the sperm whale clicks), which is larger than other comparable measurements of the TS of a single squid of this size. Madsen *et al.* (2007) consider lower TSs for head-on exposures, in the range of -70 to -60 dB. The TS of fish species depends on the size and presence of a swim bladder. For bladderless fish, a TS = $-47 \text{ dB} + 10\log_{10}(L^2/1 \text{ m}^2)$ dB ~ -47 dB is expected for a fish length $L = 1$ m, with somewhat higher TSs for fish with swim bladders, TS = $-29 \text{ dB} + 10\log_{10}(L^2/1 \text{ m}^2)$ dB ~ -29 dB (Ainslie, 2010).

A range of TS from -40 dB (“high TS” scenario) and TS = -60 dB (“low TS” scenario) was used to cover a reasonable range of expected TS in prey types that sperm whales encounter during their foraging dives. The model parameters

used to assess the masking potential under normal conditions and during sonar exposures are summarized in Table II.

III. RESULTS

A. Masking during natural ambient noise conditions (dominated by wind-generated noise from the sea surface)

In situations where echolocating sperm whales are competing against wind-generated ambient sound during their echolocation, the model predicted that the SNR exceeded the detection thresholds beyond the maximum inspection range as determined by ICIs (Fig. 4) under optimal conditions (facing away from the source and transmitting with high ESL at a prey with high TS). For a reasonable range of wind conditions, the masking model suggested that sperm whale detection of prey echoes at depth while facing 90°

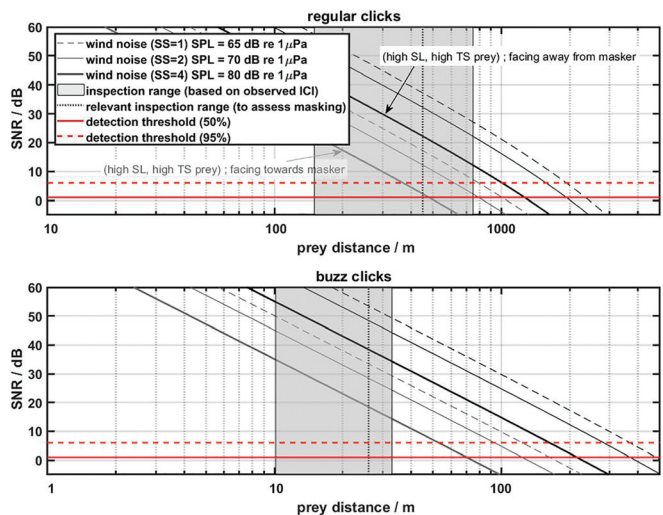


FIG. 4. Modeled prey echo SNR as a function of prey distance for regular clicks (top) and buzz clicks (bottom) for different ambient noise conditions (SS = 1, 2, and 4 and SPL within the 13.4 ± 1.8 kHz band). The gray area indicates the inspection range corresponding to the observed ICIs for regular sperm whale echolocation clicks after prey capture attempts (Fais *et al.*, 2015) and during buzzes (Isojunno and Miller, 2018). Gray vertical lines indicate the relevant inspection ranges used to evaluate the masking potential. Detection thresholds are indicated in red (solid: 50% detection probability, dashed: 95% detection probability). In this example, high ESL and TS were assumed at 50% and 95% detection thresholds while the animal was assumed to be oriented 90° away from the sea surface (i.e., high spatial masking release scenario).

away from the sea surface was not masked by wind noise unless it was transmitting at low ESL and looking for prey with low TS in conditions with SS 2 or higher (Fig. 5).

Furthermore, the model indicated that the masking potential for buzz clicks during prey capture attempts was smaller (higher SNR) than during the regular echolocation phase

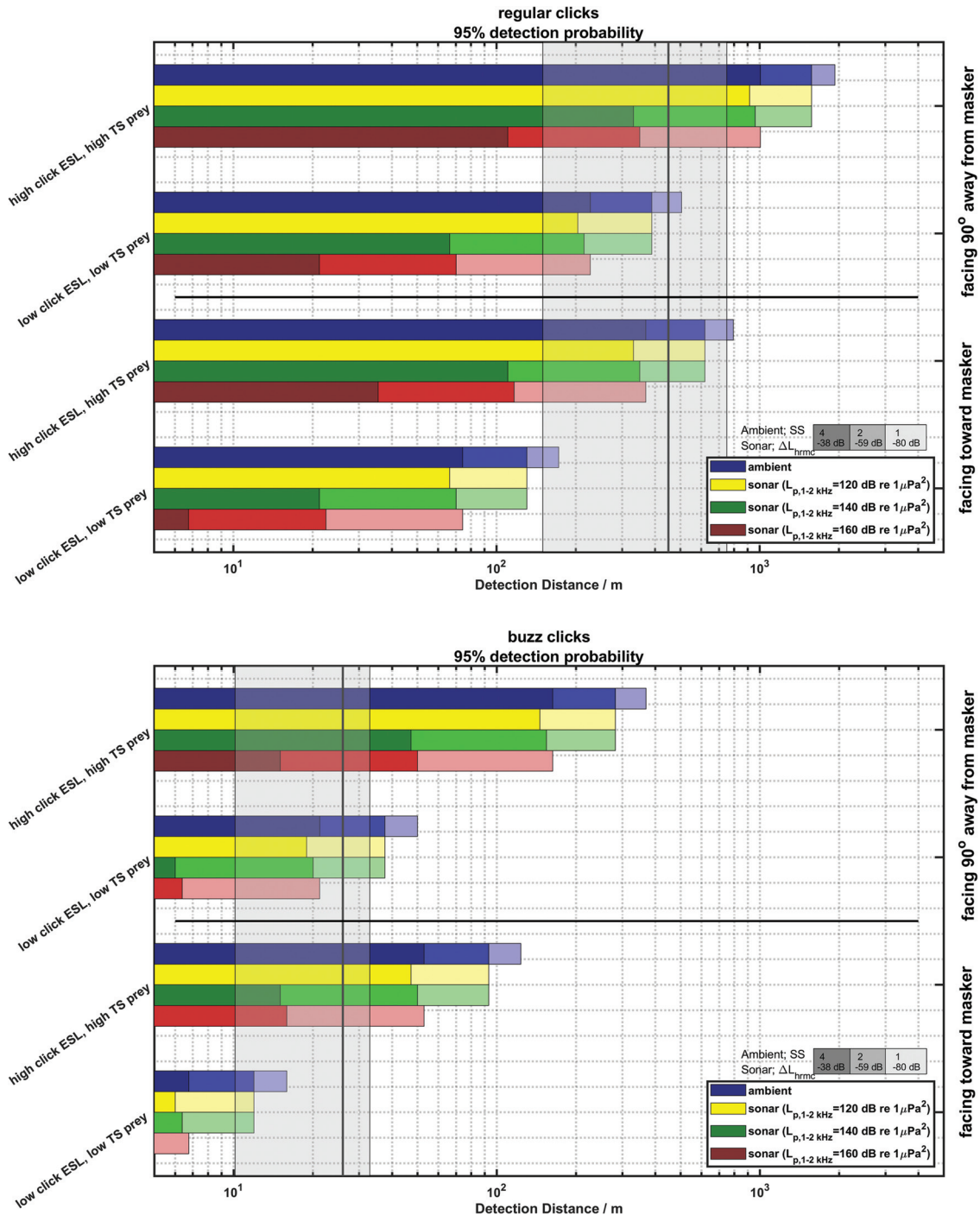


FIG. 5. Modeled detection distance (95% detection probability) for sperm whale regular (top) and buzz (bottom) clicks for different orientations between the sperm whale and masking sound, source levels, and prey TSs. The sperm whale was assumed to be facing away from the masking source (including spatial masking release, $PG_{max} = 20$ dB; left bars) or toward the masking source (no spatial masking release, $PG_{min} = 0$ dB). Masking sounds are (from top to bottom) ambient wind-driven noise and 1–2 kHz sonar with different SPL $L_{p,1-2\text{kHz}}$ (120, 140, and 160 dB re $1 \mu\text{Pa}^2$). The ambient noise scenario considered different SSs (1, 2, and 4). For the sonar scenarios, different corrections for the harmonic levels were assumed around the 13.4 kHz band compared to the 1–2 kHz band ($\Delta L_{hrmc} = -38, -59, \text{ and } -80$ dB, from dark to lighter shading). Sonar scenarios never had longer estimated detection ranges than in ambient noise conditions corresponding to SS 2. The gray area indicates the inspection range corresponding to the observed ICIs for regular sperm whale echolocation clicks after prey capture attempts (Fais *et al.*, 2015) and during buzzes (Isojunno and Miller, 2018). Gray vertical lines indicate the mean relevant inspection ranges, derived from observed ICIs, used to evaluate masking potential. Note that for some sonar exposure scenarios, detection ranges were limited by the ambient noise instead of sonar harmonic levels, in which case only detection distances are visible for higher ΔL_{hrmc} .

(Figs. 4 and 5) despite the lower ESL. When the animal was facing toward the sea surface (masker) and thus the animal would not benefit from spatial masking release, the model indicated that sperm whales could still detect high TS prey when transmitting at high ESL (Fig. 5). Masking conditions were met, however, for low TS when transmitting at low ESL when directed toward the sea surface.

B. Masking potential during sonar exposure

The predicted masking potential during sonar exposure was strongly dependent on the levels of the sonar harmonics in the sperm whale echolocation band, which were a function of SPL in the 1–2 kHz band, and the relative amount of energy in the harmonics (Fig. 5). Differences in the modeled masking potential in Fig. 5 and the influence of the adopted

	Regular clicks				Buzz clicks			
	Oriented away from masker (90°)		Oriented towards masker (0°)		Oriented away from masker (90°)		Oriented towards masker (0°)	
	High click ESL, high TS	Low click ESL, low TS	High click ESL, high TS	Low click ESL, low TS	High click ESL, high TS	Low click ESL, low TS	High click ESL, high TS	Low click ESL, low TS
Wind noise								
SS=1	Green	Yellow	Green	Orange	Green	Green	Green	Orange
SS=2	Green	Orange	Yellow	Red	Green	Green	Green	Orange
SS=4	Green	Orange	Orange	Red	Green	Orange	Green	Red
Sonar								
$L_{p,1-2kHz} = 120 \text{ dB re } 1 \mu\text{Pa}^2$								
$L_{hmc} = -80 \text{ dB}$	Green	Orange	Yellow	Red	Green	Green	Green	Orange
$L_{hmc} = -59 \text{ dB}$	Green	Orange	Yellow	Red	Green	Green	Green	Orange
$L_{hmc} = -38 \text{ dB}$	Green	Orange	Orange	Red	Green	Orange	Green	Red
Sonar								
$L_{p,1-2kHz} = 140 \text{ dB re } 1 \mu\text{Pa}^2$								
$L_{hmc} = -80 \text{ dB}$	Green	Orange	Yellow	Red	Green	Green	Green	Orange
$L_{hmc} = -59 \text{ dB}$	Green	Orange	Orange	Red	Green	Orange	Green	Red
$L_{hmc} = -38 \text{ dB}$	Orange	Red	Red	Red	Orange	Red	Orange	Red
Sonar								
$L_{p,1-2kHz} = 160 \text{ dB re } 1 \mu\text{Pa}^2$								
$L_{hmc} = -80 \text{ dB}$	Green	Orange	Orange	Red	Green	Orange	Green	Red
$L_{hmc} = -59 \text{ dB}$	Orange	Red	Red	Red	Green	Red	Orange	Red
$L_{hmc} = -38 \text{ dB}$	Red	Red	Red	Red	Orange	Red	Red	Red

FIG. 6. Summary of masking model predictions for regular (left) and buzz (right) echolocation clicks, showing the masking potential for the different scenarios. Color coding of the masking potential was based on the modeled detection distance relative to inspection ranges derived from ICIs. Green: detection distance exceeded the largest inspection ranges, indicating the lowest potential for masking; yellow: detection distance exceeded mean inspection range but was smaller than the largest inspection ranges; orange: detection distance was smaller than the mean inspection range but larger than the minimum inspection range; red: detection range was smaller than the minimum inspection range, indicating the greatest potential for masking.

relevant inspection range were more readily seen when the scenarios were color coded by the relation of the modeled detection distances to observed inspection ranges (Fig. 6).

In the case of an animal facing toward the masking sonar source, sperm whale regular echolocation was predicted to be masked at received levels of $L_{p,1-2\text{kHz}} = 160 \text{ dB re } 1 \mu\text{Pa}^2$, even for the lowest harmonic content ($\Delta L_{\text{harmc}} = -80 \text{ dB}$). For $L_{p,1-2\text{kHz}} = 120 \text{ dB re } 1 \mu\text{Pa}^2$, masking occurred when facing the sonar if strong harmonic content was present ($\Delta L_{\text{harmc}} = -38 \text{ dB}$). Masking was predicted to occur for exposures at $L_{p,1-2\text{kHz}} = 140 \text{ dB re } 1 \mu\text{Pa}^2$, only when high levels of harmonics were present (-38 dB relative to the 1–2 kHz band).

In the optimal case for the foraging sperm whale facing away from the source of masking noise and transmitting high ESL and looking for prey with high TS, echoes from regular clicks were predicted not to be masked at $L_{p,1-2\text{kHz}} = 120 \text{ dB re } 1 \mu\text{Pa}^2$, even for the highest harmonic levels. For low ESL and low TS prey, a strong reduction in detection distances occurred for all sonar SPLs, as was also seen for detection in ambient noise conditions (Fig. 5).

The masking potential of sonar was predicted to be lower for buzzes than for regular clicks. For an animal facing away from the sonar source, transmitting at high ESL, and targeting high TS prey, buzz clicks were only predicted to be masked over the search distance at the highest sonar exposures $L_{p,1-2\text{kHz}} = 160 \text{ dB re } 1 \mu\text{Pa}^2$ with high harmonic content ($\Delta L_{\text{harmc}} = -38 \text{ dB}$). When the animal transmitted at low ESL and targeting low TS prey, it was masked when $L_{p,1-2\text{kHz}} = 120 \text{ dB re } 1 \mu\text{Pa}^2$ with high harmonic levels ($\Delta L_{\text{harmc}} = -38 \text{ dB}$) and for $L_{p,1-2\text{kHz}} = 140 \text{ dB re } 1 \mu\text{Pa}^2$ with medium harmonic levels ($\Delta L_{\text{harmc}} = -59 \text{ dB}$). When facing toward the sonar, buzz clicks with high ESL and high TS prey were predicted to be masked for $L_{p,1-2\text{kHz}} = 140 \text{ dB re } 1 \mu\text{Pa}^2$ and the presence of high harmonic levels ($L_{\text{harm}} = -38 \text{ dB}$). The masking for buzz clicks was never predicted to be continuous at $L_{p,1-2\text{kHz}} = 160 \text{ dB re } 1 \mu\text{Pa}^2$, as detection distances for low harmonic levels ($L_{\text{harm}} = -80 \text{ dB}$) still exceeded the relevant inspection range.

IV. DISCUSSION

To investigate the masking potential of continuous and pulsed active sonar sounds for echolocating sperm whales, a masking model was developed for their regular search phase and buzz phase associated with prey capture attempts in varying masking noise conditions. For the evaluation of the masking potential of sonar, sonar exposure conditions like those during the 3S3 controlled exposure experiments with sperm whales (Isojunno *et al.*, 2020) were considered. This study aimed to provide a realistic range of scenarios for sperm whales based on what is known about the echolocation capabilities of other echolocating odontocetes.

A. Masking potential of continuous and pulsed active sonar of sperm whale echolocation

Conditions where masking would continuously occur throughout a sonar exposure (regardless of varying

harmonic content) for an animal facing the sonar were predicted for received sonar SPLs of $L_{p,1-2\text{kHz}} = 160 \text{ dB re } 1 \mu\text{Pa}^2$. At these levels, the model indicated that continuous masking of prey items at typical inspection ranges would occur during its regular echolocation clicking, but buzz clicks would only be partially masked (during periods when high harmonic levels are reached). Depending on sperm whale click ESL, its orientation, and TS of the prey, masking was predicted to occur for levels down to $L_{p,1-2\text{kHz}} = 120 \text{ dB re } 1 \mu\text{Pa}^2$, but unlikely to be continuous, as harmonic content was varying throughout the exposures (Fig. 5).

Sonar exposures with $L_{p,1-2\text{kHz}}$ exceeding $160 \text{ dB re } 1 \mu\text{Pa}^2$ were measured during the controlled exposure experiments (Isojunno *et al.*, 2020). The highest levels of up to $L_{p,1-2\text{kHz}} = 180 \text{ dB re } 1 \mu\text{Pa}^2$ were only achieved for PAS signals during the on-time (1 s) of the transmission and dropped quickly by approximately 20 dB 1 s after the end of the PAS direct arrival and by 30 dB for 3 s after the exposure (Fig. 1). The longer CAS signals (19 s) were transmitted at the same ESL as the PAS signals; thus, the highest SPL for CAS signals tended to average 14 dB lower than for PAS signals. However, CAS exposures had a higher percentage of time above the masking threshold throughout each pulse cycle due to their near-continuous transmission (Fig. 1). This indicated that the masking potential of CAS signals was higher than PAS overall, at least at the levels achieved during these behavioral experiments (Isojunno *et al.*, 2020).

Sonar levels predicted to mask sperm whale echolocation ranged from $L_{p,1-2\text{kHz}} = 160 \text{ dB re } 1 \mu\text{Pa}^2$ (continuous masking for an animal facing the sonar) down to $L_{p,1-2\text{kHz}} = 120 \text{ dB re } 1 \mu\text{Pa}^2$ (occasional masking for an animal facing the sonar) but strongly depended on the orientation of the animal and assumptions about the source level and TS of the prey items it was echolocating upon. The range of levels found to mask echoes in the main sperm whale echolocation frequency band were comparable to those associated with behavioral changes in sperm whales, such as cessation of deep foraging dives (Miller *et al.*, 2012) and switching to active non-foraging behavior (Isojunno *et al.*, 2016; Isojunno *et al.*, 2020), which were observed in the range of $L_{p,1-2\text{kHz}} = 120\text{--}170 \text{ dB re } 1 \mu\text{Pa}^2$. For these experiments, the model indicated that masking of echolocation would occur at source-to-animal distances similar to, but not necessarily larger than, those for which behavioral disturbance has been observed. Due to the varying harmonic levels and varying orientation of the sperm whales relative to the sonar, the model suggested that masking was unlikely to be continuous throughout the CAS exposures in the Isojunno *et al.* (2020) experiments.

Extrapolation of these model predictions to other sound sources and larger distances should consider differences in main sonar frequency, source level, and harmonic content of the source spectrum. The 1–2 kHz frequency range of the sonar considered here is relatively low for active sonar systems used to detect submarines (D'Amico and Pittenger, 2009). Fixed ratios between the 1–2 kHz and the sperm

whale effective detection band ΔL_{hrmc} were considered in this study. The high received levels ($L_{p,1-2\text{kHz}} \geq 160 \text{ dB re } 1 \mu\text{Pa}^2$) recorded on sperm whales during the 3S3 controlled exposure study (Isojunno *et al.*, 2020) were achieved during approaches within 1–7 km. At these distances, the relative difference in attenuation in water at these two frequency bands is limited. For higher source levels and increasing distances at which the same sonar received levels are achieved, absorption in the water will cause greater attenuation at higher frequencies, changing the level difference between the main sonar band and the sperm whale echolocation band. For example, the change in received level in the area of the 3S3 experiments suggested a $15 \log_{10}(r/r_{\text{ref}})$ falloff with range (mode-stripping regime; Weston, 1971). Therefore, for a sonar source with a source level of 220 dB re $1 \mu\text{Pa}^2 \cdot \text{m}^2$ (6 dB higher than used in the experiment) the distance at which the $L_{p,1-2\text{kHz}}$ is achieved would increase by a factor of 2.3 (assuming mode-stripping and frequency-dependent absorption), whereas the increase is smaller (factor of 1.45) at 13.4 kHz due to the increased sound attenuation at higher frequencies. In that situation, the masking potential for sperm whale echolocation would be lower at the same $L_{p,1-2\text{kHz}}$.

Our results suggested that the masking potential was higher during regular clicking in the search phase than during buzzes associated with prey capture attempts. At first sight, this may appear somewhat counter-intuitive, since the sperm whales drastically reduce the ESL of buzz clicks by almost 30 dB compared to search clicks. This reduction in ESL may be to reduce forward masking, be driven by limitations in the pneumatically driven sound production of series of clicks, or serve to simplify the auditory scene by reducing the amount of prey echoes and reverberation from larger distances (Tønnesen *et al.*, 2020). The higher SNRs in our model for prey echoes during a buzz are a consequence of the much-reduced two-way propagation loss since the animal is aiming at much closer prey. Some buzz clicks appear to be more broadband and centered at higher frequencies than assumed in this study (Fais *et al.*, 2016), which would also further reduce the masking potential during the buzz phase.

During ambient noise limited conditions, the model suggested that sperm whales can detect prey items within their inspection range based upon ICIs. This is not unexpected, as this represents the natural conditions in which the sperm whale evolved its echolocation strategy. The model indicated that in conditions when the animal faces directly upward, where most of the masking noise is coming from, and when transmitting at relatively low source levels and targeting low TS prey, prey echoes may be masked. Analysis of the tagged sperm whale data reported in Isojunno *et al.* (2020) indicated that during the layer-restricted search phase, 62% and 94% of tagged sperm whales started regular click trains with a pitch $< 0^\circ$ and $< 30^\circ$, respectively (based on $N = 15$ individuals, 4756 click trains, during baseline conditions). This indicates that sperm whales have a tendency to echolocate facing horizontally or facing down. Nevertheless, occasional clicking during

ascent has been observed. Studies of tagged sperm whales echolocating in different weather conditions may help to elucidate whether upward-facing sperm whales show anti-masking strategies or whether sperm whales spend more time facing away from the sea surface whilst echolocating in higher noise conditions predicted by the model.

B. Significance of masking

Our assessment of the masking potential was based on the assumption that masking is significant when detection distances fall below typical inspection ranges. We cannot be certain of the degree to which the foraging ability of sperm whales would be affected if such masking did occur. The large and stable ICI for sperm whales during the regular clicking is suggested to facilitate acoustic scene analysis. Maintaining high click source level, which may require air recycling (Isojunno and Miller, 2018), indicates that click source level is not directly related to the effective distance at which prey echoes are targeted by the sperm whale (Tønnesen *et al.*, 2020). For this reason, we considered the inspection range after prey capture attempts, which are likely representative of the maximum distance over which sperm whales search for food during their foraging dives (Fais *et al.*, 2015), and for distances at which sperm whales are believed to switch to the buzz phase (Fais *et al.*, 2016; Tønnesen *et al.*, 2020).

Estimating effective distances of prey items using DTAGs, as done for beaked whales and porpoises (Johnson *et al.*, 2004; Wisniewska *et al.*, 2016), is challenging with sperm whales due to tag placement and acoustic shadowing by the animals' bodies, but this has recently been achieved on a single young sperm whale foraging at the lower latitudes of the Azores archipelago (Tønnesen *et al.*, 2020). For this individual, echolocation click echoes detected on the DTAG indicate that the animal foraged in areas with lower prey densities and switched from regular echolocation to a buzz at roughly 2 times its body length. This is a distance somewhat larger than that for smaller odontocetes and that previously estimated in Fais *et al.* (2016) for sperm whales, and it is argued by Tønnesen *et al.* (2020) that this may be a result of the powerful biosonar enabling larger detection distances combined with possibly a limited maneuverability of the large-bodied sperm whale. Effective distances can also be indirectly measured from buzz rates measured during foraging dives (Teloni *et al.*, 2008). Teloni *et al.* (2008) estimated that sperm whales encounter a prey item every 65 m during deep dives and every 190 m during shallow dives. They also suggest the possibility that sperm whales target multiple prey items during long buzzes while deep diving. Comparison of these distances to masked detection distances (Fig. 5) suggests that under some conditions (high harmonic content or animal facing the sonar), masked detection distances fall below these estimated prey distances intermittently (when high harmonic levels are reached). In a situation when relatively few prey echoes are present, occasional periods of masking for periods with high harmonic content

may still be biologically significant as they may coincide by chance with the arrival of prey echoes.

C. Masking model uncertainties and knowledge gaps

Clearly, a large knowledge gap for the analysis was the lack of measurements on hearing capabilities of sperm whales, as hearing integration time, masked detection thresholds, and hearing directionality have not been measured in this species. Hence, there are inherent uncertainties present in the masking potential estimated in our study. Although sperm whales are part of the odontocete suborder, they have evolved a different sound production mechanism and somewhat different middle and inner ear structure than those of smaller odontocete species, such as the killer whales and dolphins (Wartzok and Ketten, 1999; Southall *et al.*, 2019). Therefore, some care should be taken when extrapolating information on the biosonar function between odontocete species.

Several of the better-studied model parameters in this study are known to be variable. This was accounted for by considering a range of optimistic to pessimistic scenarios to understand under what conditions masking of prey echoes could occur. The range of click on-axis ESLs measured in high-latitude whales (Madsen *et al.*, 2002) was used to investigate a range of possible source levels that may occur in nature. Due to the high directionality of odontocete echolocation clicks (Møhl *et al.*, 2003; Zimmer *et al.*, 2005; Jensen *et al.*, 2018) and the difficulty of measuring exactly on-axis of the sperm whale, our assumption of the on-axis level may slightly underestimate the actual ESLs. Click source levels may also depend on body size and hence be smaller for female and juvenile sperm whales present at lower latitudes (Tønnesen, 2020). A decrease in apparent source levels and changes in frequency spectrum of buzz clicks with depth were reported by Isojunno and Miller (2018), but depth-dependence of source level was not found in measured on-axis clicks (Madsen *et al.*, 2002). Such apparent depth-dependencies may be explained by changes in beam width associated with the buzz phase. For instance, harbor porpoises have been shown to be able to adjust their beam width adaptively (Wisniewska *et al.*, 2015). Hence, these apparent depth-dependencies may not represent a true decrease in on-axis source level (Isojunno and Miller, 2018).

The TSs considered in this study were based on measured TS of individual prey items. Less information is available on the prey patches, which could be used by sperm whales while searching for prey. Echoes of presumed prey patches have been reported for a sperm whale foraging in low-latitude environments (Tønnesen, 2020). Such prey patches could lead to higher TSs as they consist of multiple animals (Love, 1981; André *et al.*, 2007).

The estimates for masking distances presented in this study are based on detection thresholds measured in dolphins, where the animals were trained to indicate whether a known target was present or absent. The DT95 adopted in this study was derived from observations with multiple

captive dolphins (Au, 1993, 2014), but it is known that variability in detection threshold exists between species and individuals within species (e.g., Au *et al.*, 1987; Turl *et al.*, 1987). It is likely that higher SNRs are required for an animal to distinguish between echo features than to just detect the presence of an echo. For instance, jitter studies with bats show that under masked conditions, the ability to measure time differences of 232 μ s is approximately random at SNR of \sim 0 dB, increases to 70% performance at 9.5 dB, and increases further to 90% for SNR $>$ 20 dB (Simmons, 2017). Echolocation studies in captive and wild odontocetes suggest that spectral and fine-scale temporal information is used by the animals to discern between objects and prey types (e.g., Au *et al.*, 1980; Branstetter *et al.*, 2007; Jones *et al.*, 2008; Kloepper *et al.*, 2018). To our knowledge, no studies have looked at target discrimination under masked conditions in odontocete species, making it hard to quantify at what SNRs this might occur. A masking study that was aimed at partially filtering the frequency content of echo clicks shows that dolphins use the full bandwidth of the click that is audible for detecting clicks (Ibsen *et al.*, 2009; Ibsen *et al.*, 2011). Although a wider frequency band than the effective detection bandwidth ratio Q_{eff} considered here is used by the animals to detect prey, we focused on a Q_{eff} around the centroid frequency because it required the least amount of extrapolation from the study (Au, 2014) from which the DT was derived. This represented our best estimate of scenarios for which a sperm whale is no longer able to detect echoes. Energy at lower frequencies that would have a stronger contribution from sonar harmonics may be used by the animal. However, Ibsen *et al.* (2011) showed that echolocating bottlenose dolphins and a false-killer whale (*Pseudorca crassidens*) primarily used frequencies within the dominant energies of the clicks (roughly frequencies with spectral amplitudes exceeding 80% of the maximum spectral amplitude) for target detection. For the sperm whale click considered here, an 80% criterion would correspond to a frequency range of 11.5–16 kHz, which is only a factor of 2.5 greater than the effective detection bandwidth considered here.

One critical question is whether the detection thresholds adopted in this study, which were measured (Au, 2014) using broadband masking sounds, are representative for tonal masking sounds such as sonar sounds. For longer duration tonal sounds, it is known that various processes, such as comodulated masking release, dip-listening, and harmonic analysis of broadband signals, allow animals to detect signals in natural masked conditions compared to Gaussian noise masking conditions (Erbe, 2008; Branstetter *et al.*, 2008; Trickey *et al.*, 2010; Branstetter *et al.*, 2013; Cunningham *et al.*, 2014). However, to our knowledge, the ability of tonal sounds to mask detection and recognition of short broadband clicks has not been directly investigated. To better understand the effect of tonal masking on the detection and recognition of broadband echolocation click echoes, studies are required to quantify target detection and discrimination under tonal masked conditions.

An important aspect of the biosonar system, neglected in this study, is the presence of an automatic gain control (AGC) in the animal's auditory system, which has been shown to occur in false-killer whales, bottlenose dolphins (Ya Supin and Nachtigall, 2013; Finneran *et al.*, 2013), and harbor porpoises (Linnenschmidt *et al.*, 2012; Ladegaard, 2017). This AGC consists of two mechanisms, a forward masking response to the echolocation signal emitted by the animal and a change of the baseline hearing threshold with time, since a click was emitted that can be adapted to the target distance (Ya Supin and Nachtigall, 2013). The AGC has likely evolved to deal with a large dynamic range of prey echoes at different distances and to keep expected prey echo levels from different prey distances within a range that is optimal for perception (Ya Supin and Nachtigall, 2013; Ladegaard, 2017). Auditory evoked potential (AEP) measurements decreased with 40 dB within the first 16 ms after the emission of a click, which then leveled off to a constant hearing sensitivity. It is difficult to compare these forward-masked thresholds to the masking noise levels expected from ambient and sonar noise levels. The time for recovery of the forward masking of approximately 16 ms corresponds to roughly 12 m prey distance, and hence the echo SNR predicted here may be underestimated in our model at very short prey distances during regular echolocation. It is possible that the forward masking is also reduced during the buzz phase as a consequence of the reduction of click ESL.

The masking potential of various levels of harmonic content of the 1–2 kHz sonar in the echolocation band was modeled. Studies of upward-masking in humans (Egan and Hake, 1950) and one study of one dolphin (Johnson, 1971) indicate that intense low frequency exposures can mask or suppress hearing sensitivity at higher frequencies due to the nonlinear behavior of the basilar membrane (Oxenham and Plack, 1998; Branstetter *et al.*, 2008). A lack of understanding of the upward-masking mechanism precluded incorporating this process into our quantitative model. Based on what is observed in humans (Egan and Hake, 1950), upward masking to frequencies significantly higher than the masker frequency (e.g., a factor 10) is expected to occur only at relatively high (~80 dB) sensation levels (i.e., the amount in decibels that a stimulus is above the hearing threshold). Sensation levels of the sonar signals for sperm whales could not be estimated due to a lack of reliable hearing sensitivity measurements in this species.

D. Animal orientation and masking release mechanisms

Our investigation of the scaling relation of masking release and directional hearing sensitivity with head size indicated that the greatest masking release tended to occur at frequencies that coincided with click centroid frequencies. This pattern appeared to hold for a range of echolocating odontocetes that vary in body size, from harbor porpoises to killer whales (Fig. 3). The centroid wavelengths of echolocation clicks corresponded to roughly 10–25 times the head size. Head size was used for the scaling, as it was

considered a good proxy for head shielding, which likely plays an important role in hearing directionality at higher frequencies. An alternative would be to use the distance between the inner ears (or distance between pan bones as a proxy), which may be more related to inter-aural time differences that mediate hearing directionality at lower frequencies. However, since information on these distances is lacking in the literature, head size was used for practical considerations.

To obtain data for a large range of odontocete species, we pooled data based on masking release studies with directional hearing studies. Although the data points from a study of dolphins and beluga were not based on masking release studies, measurements for bottlenose dolphins (Au and Moore, 1984; Popov and Supin, 2009; Popov *et al.*, 2020) suggested that the directionality of hearing increased with frequency in a similar fashion as did the masking release. This indicated that the receiving beam pattern of an animal for the masking sounds affected the amount of masking release, which was the reason for including these data points in this study. Although the scaling relation in Fig. 3 showed some scatter, extrapolating the observed trend to the centroid frequency and head size of sperm whales, our best estimate for the sperm whale degree of masking release was in a range of 13–24 dB. For this reason, the maximum spatial masking release of $PG_{max} = 20$ dB assumed in this study seemed a reasonable estimate for masker sources located at 90° from the animal and was in line with assumptions made in previous studies estimating detection distances for sperm whales (Madsen *et al.*, 2007).

Generic scenarios where the animal was facing toward and away from the masker were adopted, in which the maskers were considered as sources with a discrete direction situated at an angle of 0° or 90° from the echolocating sperm whale. In reality, the masking sound will not arrive at the animal from just one direction, but rather from different angles as a result of reflections and refraction in the deep waters where sperm whales forage. Reverberation will occur over a wider range of angles, effectively reducing the levels within different angles compared the levels measured on the hydrophone on the tagged animals (Fig. 1). Models are available that can quantify the distribution of sound arriving from different angles, which depends strongly on the environmental conditions (sound speed profile, sea surface roughness, bottom topography, and seafloor type), depth of the animal, and frequency, depth, and directionality of the transmitting sound source (e.g., Porter and Reiss, 1984; Porter and Bucker, 1987; Collins, 1993). However, to include this effect in a masking prediction also requires more detailed knowledge of the spatial masking release in these animals than is currently available. High-frequency ambient noise in deep waters tends to be concentrated in angles to the sea surface (Short, 2005; Barclay and Buckingham, 2013). Sperm whales foraging in a prey layer normally swim horizontally through different prey patches (Guerra *et al.*, 2017; Isojunno and Miller, 2018; Tønnesen, 2020); hence, the assumption that the masking sound is

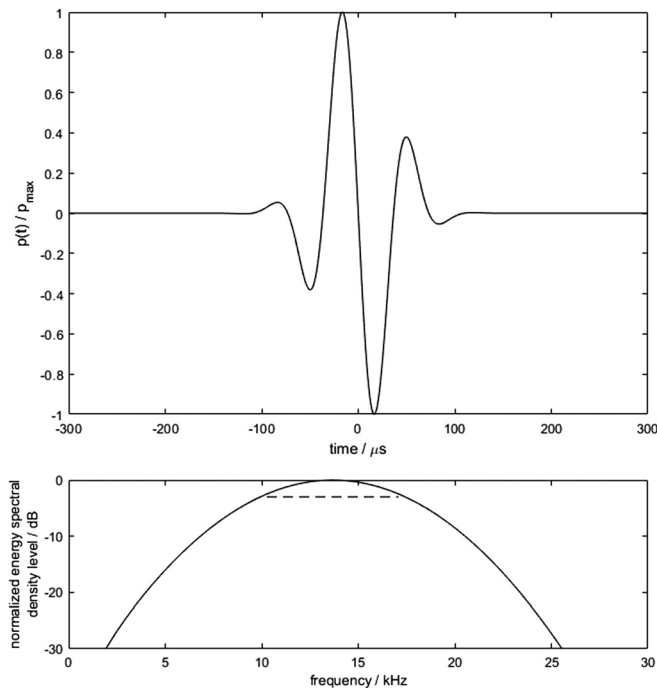


FIG. 7. (Color online) Approximation of a sperm whale echolocation click using a Gabor wavelet with parameters chosen so as to provide a similar centroid frequency and -3 dB bandwidth as the sperm whale clicks presented in Madsen *et al.* (2002) and Møhl *et al.* (2003). Top panel: normalized simulated sperm whale click pressure waveform $p(t)/p_{\max}$. Bottom panel: Spectrum of the simulated sperm whale click waveform. This waveform was used to estimate the energy within the effective band in which the detection threshold was defined. The pattern and duration and the corresponding spectrum are quite similar to those of actual regular on-axis sperm whale clicks presented in Madsen *et al.* (2002). Based on this, the energy was estimated to be -5 dB of the total click energy.

approximately at 90° is reasonable for ambient sound. Sperm whales do occasionally face upward toward the sea surface whilst echolocating. In such a situation, it is likely that masking release experienced by the animal will lie somewhere between no release (assuming all wind noise is located in a direction directly in front of the animal) and the level of release experienced when the animal is moving horizontally.

Sperm whales occasionally feed close to the sea floor (Watwood *et al.*, 2006; Teloni *et al.*, 2008; Guerra *et al.*, 2017; Isojunno and Miller, 2018; Tønnesen, 2020). In such situations, reverberation caused by the seafloor may also add to the natural masking potential (Ainslie, 2010). Reflections of echolocation clicks from the seafloor can regularly be observed on DTAGs attached to diving sperm whales (e.g., Zimmer *et al.*, 2005). Sperm whales observed to forage near the sea floor showed a tendency to swim upside-down, which may serve to reduce reflections from the seafloor or as a strategy to hunt for benthic prey whilst protecting their mouth (Tønnesen, 2020). Scattering from other animals in the prey layers will also contribute to reverberation; the degree to which this contributes to the masking potential is likely to be dependent on the prey density and surface scattering strength. The effect of reverberation on the sperm whale’s ability to detect echoes was not considered in this study but can be included using reverberation

modeling (e.g., Ainslie *et al.*, 1996; Ainslie, 2010). However, this needs to consider the effect of directionality of the outgoing click as well as the hearing directionality. Modeling the masking potential from the click reverberation or distributed masking sound due to multipath and reverberation structure of sonar sound would require a measurement or model of the full angle-dependent form of the masking release. In this study, we found for several odontocete species that animal head size appeared to scale with the amount of spatial masking release for a masker at 90° . Future studies could explore whether this scaling relationship can be generalized to other angles and larger species such as the sperm whale. However, this requires spatial masking release studies in several species over a wider range of angles and an improved theoretical understanding of how the hearing directionality functions in odontocetes.

Toothed whales show high adaptability to masking conditions, such as increasing the levels of the transmitted signals (Lombard effect), shifting frequency outside frequencies containing masker noise, or increasing click rates (Au *et al.*, 1974; Au *et al.*, 1985; Moore and Pawloski, 1990; Thomas and Turl, 1990; Romanenko and Kitain, 1992). Investigation of responses to controlled sonar exposures may indicate whether sperm whales in different stages of their foraging dives adopted such anti-masking strategies in situations of high potential masking conditions. Potential signs of anti-masking strategies could involve orientation away from the source while foraging, as spatial masking release was predicted to have a significant reduction in masking potential, but also increase in click ESL or reduction of inspection range (ICI) to compensate for increased noise levels. Other factors such as reduced foraging efficiency should also be considered. Responses are more likely to occur during the regular search phase than during the buzz phase since a higher masking potential was predicted for regular clicks.

Sperm whales produce other broadband clicks, such as codas, slow clicks, and rasps, which are used for communication with other conspecifics (Watkins and Schevill, 1977; Rendell and Whitehead, 2003; Madsen *et al.*, 2002; Oliveira *et al.*, 2013). The frequency content of communication clicks is lower, with peak frequencies of coda clicks around 5 kHz (Madsen *et al.*, 2002), and more omnidirectional, which likely serves for long range communication. The lower frequencies lead to a stronger overlap of the sonar signals and higher harmonics with the communication signals and hence would merit a separate investigation into the masking potential, which is left for future work.

V. CONCLUSION

Modern active sonar systems can continuously transmit and receive sound, which can lead to increased masking of sounds perceived by marine mammals compared to the intermittent sounds of traditional sonars. To support the interpretation of behavioral responses of sperm whales to continuous and pulsed active sonar (Isojunno *et al.*, 2020),

this study investigated the potential of 1–2 kHz active sonar and its harmonic content at higher frequencies to mask echolocation echoes used by sperm whales in high-latitude areas. The masking potential was investigated by modeling the echolocation detection process in sperm whales. The masking potential predicted by the model varied strongly with different scenarios considered (Fig. 6).

Sonar levels predicted to mask sperm whale echolocation ranged from $L_{p,1-2\text{kHz}} = 160$ dB re $1 \mu\text{Pa}^2$ (continuous masking for an animal facing the sonar) down to $L_{p,1-2\text{kHz}} = 120$ dB re $1 \mu\text{Pa}^2$ (intermittent masking for an animal facing the sonar) but strongly depended on the orientation of the animal relative to the masker, click source level, and TS of the prey items it was echolocating upon. For sonar exposures as occurred during the 3S3 controlled exposure experiments (Isojunno *et al.*, 2020), the model predicted only a few conditions where masking would be expected to occur continuously.

The masking model predicted that echoes from buzz clicks were less likely to be masked than echoes from regular clicks, even though the ESL is much lower for buzz clicks than for the regular clicks. This was because the reduction in echo level due to lower source levels of buzz clicks was more than compensated for by the reduced two-way travel distance to nearby prey being buzzed at and corresponding lower propagation losses.

When reviewing the literature to build this masking model, several key knowledge gaps were identified. No studies exist on the masking potential of tonal sounds on the detection of echoes and the classification of target types, which may be different from broadband Gaussian noise typically used during masking studies. Furthermore, upward-masking studies that investigate the interference of loud low frequency sounds with the detection of higher frequency sounds are needed. These mechanisms could be investigated using target detection studies with smaller odontocetes that can be kept in captivity, which would be valuable for understanding the masking potential of sonar sounds and other loud tonal noise sources on echolocation marine mammal species. Finally, more insight is required into what distances from prey masking affect sperm whale foraging efficiency and to what extent these animals are able to adapt their biosonar to reduce masking.

ACKNOWLEDGMENTS

We thank the 3S3 scientific team and RV HU Sverdrup II captain and crew. Furthermore, we thank Sander van IJsselmuide for carrying out measurements used for the analysis of the harmonic content of the Socrates sonar sources. This study was sponsored by the U.S. Living Marine Resources program, Office of Naval Research (ONR) Grant Nos. N00014-18-1-2062 and N00014-20-1-2709, UK Defence Science and Technology Laboratory (DSTL), French Direction générale de l'armement (DGA), and the Netherlands Ministry of Defence.

APPENDIX

To estimate the amount of energy within the effective detection bandwidth of the sperm whale click, a correction factor was estimated by approximating the pressure waveform $p(t)$ of the sperm whale click with a Gabor wavelet:

$$p_{\text{Gabor}}(t) = e^{(-t^2/(2\sigma)^2)} \cdot \cos(\omega \cdot (t - t_0) + \varphi),$$

with t the time, $\sigma = 25 \mu\text{s}$, $\varphi = \pi/2$ rad, $\omega = 85\,900$ rad/s, with the same centroid frequency and -3 dB bandwidth (Fig. 7). These parameters resulted in a broadband click with a similar centroid frequency and -3 dB bandwidth as the sperm whale clicks presented in Madsen *et al.* (2002) and Møhl *et al.* (2003). The difference between the total click energy ESL and energy within the sperm whale effective detection band ESL_{eff} in the masking model adopted in this study was 5 dB.

¹See supplementary material at <https://www.scitation.org/doi/suppl/10.1121/10.0004769> for the analysis of the high-frequency harmonic content of the Socrates 1–requery harmonic content

- Accomando, A. W., Mulsow, J., Branstetter, B. K., Schlundt, C. E., and Finneran, J. J. (2020). "Directional hearing sensitivity for 2–30 kHz sounds in the bottlenose dolphin (*Tursiops truncatus*)," *J. Acoust. Soc. Am.* **147**, 388–398.
- Ainslie, M. A. (2010). *Principles of Sonar Performance Modeling* (Springer Verlag, Berlin).
- Ainslie, M. A. (2013). "Neglect of bandwidth of Odontocetes echo location clicks biases propagation loss and single hydrophone population estimates," *J. Acoust. Soc. Am.* **134**, 3506–3512.
- Ainslie, M. A., Harrison, C. H., and Burns, P. W. (1996). "Signal and reverberation prediction for active sonar by adding acoustic components," *IEEE Proc. Radar Sonar Navig.* **143**, 190–195.
- André, M., Johansson, T., Delory, E., and Van Der Schaar, M. (2007). "Foraging on squid: The sperm whale mid-range sonar," *J. Mar. Biol. Assoc. UK* **87**, 59–67.
- Arbogast T. L., Mason, C. R., and Kidd, G. Jr. (2002). "The effect of spatial separation on informational and energetic masking of speech," *J. Acoust. Soc.* **112**, 2086–2098.
- Au, W. W. L. (1993). *The Sonar of Dolphins* (Springer Verlag, New York).
- Au, W. W. L. (2014). "Dolphin biosonar target detection in noise: Wrap up of a past experiment," *J. Acoust. Soc. Am.* **136**, 9–12.
- Au, W. W. L., Floyd, R. W., Penner, R. H., and Murchison, A. E. (1974). "Measurement of echolocation signals of the Atlantic bottlenose dolphin, *Tursiops truncatus* Montagu, in open waters," *J. Acoust. Soc. Am.* **56**, 1280–1290.
- Au, W. W. L., Ford, J. K. B., Horne, J. K., and Allman, K. A. N. (2004). "Echolocation signals of free-ranging killer whales (*Orcinus orca*) and modeling of foraging for chinook salmon (*Oncorhynchus tshawytscha*)," *J. Acoust. Soc. Am.* **115**, 901–909.
- Au, W. W. L., and Hastings, M. C. (2008). *Principles of Marine Bioacoustics* (Springer Verlag, New York).
- Au, W. W. L., and Moore, P. W. B. (1984). "Receiving beam patterns and directivity indices of the Atlantic bottlenose dolphin *Tursiops truncatus*," *J. Acoust. Soc. Am.* **75**, 255–262.
- Au, W. W. L., Moore, P. W. B., and Pawloski, D. A. (1988). "Detection of complex echoes in noise by an echolocating dolphin," *J. Acoust. Soc. Am.* **83**, 662–668.
- Au, W. W. L., Penner, R. H., Carder, D. A., and Scronce, B. (1985). "Demonstration of adaptation in beluga whale echolocation signals," *J. Acoust. Soc. Am.* **77**, 726–730.
- Au, W. W. L., Penner, R. H., and Turl, C. W. (1987). "Propagation of beluga echolocation signals," *J. Acoust. Soc. Am.* **82**, 807–813.
- Au, W. W. L., Schusterman, R. J., and Kersting, D. A. (1980). "Sphere-cylinder discrimination via echolocation by *Tursiops truncatus*," in *Animal*

- Sonar Systems* edited by R.-G. Busnel and J. F. Fish (Springer, Boston), pp. 859–862.
- Aulanier, F., Simard, Y., Roy, N., Gervaise, C., and Bandet, M. (2017). “Effects of shipping on marine acoustic habitats in Canadian Arctic estimated via probabilistic modeling and mapping,” *Mar. Pollut. Bull.* **125**, 115–131.
- Bain, D. E., and Dahlheim, M. E. (1994). “Effects of masking noise on detection thresholds of killer whales,” in *Marine Mammals and the Exxon Valdez* edited by T. R. Loughlin (Academic, San Diego), pp. 243–256.
- Barclay, D. R., and Buckingham, M. J. (2013). “Depth dependence of wind-driven, broadband ambient noise in the Philippine Sea,” *J. Acoust. Soc. Am.* **133**, 62–71.
- Bates, J. R., Grimmett, D., Canepa, G., and Tesei, A. (2018). “Incoherent sub-band averaging for improved target detection and Doppler estimation in linearly frequency modulated continuous active sonar,” *Proc. Mtgs. Acoust.* **33**(1), 055001.
- Benoit-Bird, K. J., Gilly, W. F., Au, W. W. L., and Mate, B. (2008). “Controlled and *in situ* target strengths of the jumbo squid *Dosidicus gigas* and identification of potential acoustic scattering sources,” *J. Acoust. Soc. Am.* **123**, 1318–1328.
- Branstetter, B. K., Finneran, J. J., and Houser, D. S. (2008). “Frequency and level dependent masking of the multiple auditory steady-state response in the bottlenose dolphin (*Tursiops truncatus*),” *J. Acoust. Soc. Am.* **123**, 2928–2935.
- Branstetter, B. K., Mercado, E., and Au, W. L. (2007). “Representing multiple discrimination cues in a computational model of the bottlenose dolphin auditory system,” *J. Acoust. Soc. Am.* **122**, 2459–2468.
- Branstetter, B. K., Trickey, J. S., Bakhtiari, K., Black, A., Aihara, H., and Finneran, J. J. (2013). “Auditory masking patterns in bottlenose dolphins (*Tursiops truncatus*) with natural, anthropogenic, and synthesized noise,” *J. Acoust. Soc. Am.* **133**, 1811–1818.
- Bregman, A. S. (1990). *Auditory Scene Analysis: The Perceptual Organization of Sound* (MIT Press, Cambridge, MA).
- Brumm, H., and Slabbekoorn, H. (2005). “Acoustic communication in noise,” in *Advances in the Study of Behavior* edited by P. J. B. Slater, C. T. Snowdon, T. J. Roper, H. J. Brockmann, and M. Naguib (Academic Press, San Diego), pp. 151–209.
- Clark, C. W., Ellison, W. T., Southall, B. L., Hatch, L., Van Parijs, S. M., Frankel, A., and Ponirakis, D. (2009). “Acoustic masking in marine ecosystems: Intuitions, analysis, and implication,” *Mar. Ecol. Prog. Ser.* **395**, 201–222.
- Collins, M. D. (1993). “A split-step Padé solution for the parabolic equation method,” *J. Acoust. Soc. Am.* **93**, 1736–1742.
- Cron, B. F., and Sherman, C. H. (1962). “Spatial-correlation functions for various noise models,” *J. Acoust. Soc. Am.* **34**, 1732–1736.
- Cunningham, K. A., Southall, B. L., and Reichmuth, C. (2014). “Auditory sensitivity of seals and sea lions in complex listening scenarios,” *J. Acoust. Soc. Am.* **136**, 3410–3421.
- D’Amico, A., and Pittenger, R. (2009). “A brief history of active sonar,” *Aquat. Mamm.* **35**, 426–434.
- Dent, M. L., Larsen, O. N., and Dooling, R. J. (1997). “Free-field binaural unmasking in budgerigars (*Melopsittacus undulatus*),” *Behavioral Neuroscience* **111**(3), 590–598.
- Dooling, R. J., and Leek, M. R. (2018). “Communication Masking by Man-Made Noise,” in *Effects of Anthropogenic Noise on Animals* edited by H. Slabbekoorn, R. J., Dooling, A. N., and Popper, R. R. Fay (Springer Nature, New York), pp. 1–309.
- Dunlop, R. A. (2018). “The communication space of humpback whale social sounds in wind-dominated noise,” *J. Acoust. Soc. Am.* **144**, 540–551.
- Durlach, N. (2006). “Auditory masking: Need for improved conceptual structure,” *J. Acoust. Soc. Am.* **120**, 1787–1790.
- Egan, J. P., and Hake, H. W. (1950). “On the masking pattern of a simple auditory stimulus,” *J. Acoust. Soc. Am.* **22**, 622–630.
- Erbe, C. (2008). “Critical ratios of beluga whales (*Delphinapterus leucas*) and masked signal duration,” *J. Acoust. Soc. Am.* **124**, 2216–2223.
- Erbe, C., Reichmuth, C., Cunningham, K., Lucke, K., and Dooling, R. (2016). “Communication masking in marine mammals: A review and research strategy,” *Mar. Pollut. Bull.* **103**, 15–38.
- Fais, A., Aguilar Soto, N., Johnson, M., Pérez-González, C., Miller, P. J. O., and Madsen, P. T. (2015). “Sperm whale echolocation behaviour reveals a directed, prior-based search strategy informed by prey distribution,” *Behav. Ecol. Sociobiol.* **69**, 663–674.
- Fais, A., Johnson, M., Wilson, M., Aguilar Soto, N., and Madsen, P. T. (2016). “Sperm whale predator-prey interactions involve chasing and buzzing, but no acoustic stunning,” *Sci. Rep.* **6**, 1–13.
- Finneran, J. J., Mulsow, J., and Houser, D. S. (2013). “Using the auditory steady-state response to assess temporal dynamics of hearing sensitivity during bottlenose dolphin echolocation,” *J. Acoust. Soc. Am.* **134**, 3913–3917.
- Fuller, R. A., Warren, P. H., and Gaston, K. J. (2007). “Daytime noise predicts nocturnal singing in urban robins,” *Biology Lett.* **3**, 368–370.
- Gordon, J. C. D. (1987). “Behaviour and ecology of sperm whales off Sri Lanka,” Ph.D. dissertation, University of Cambridge, Cambridge, England.
- Gross, K., Pasinelli, G., and Kunc, H. P. (2010). “Behavioral plasticity allows short-term adjustment to a novel environment,” *American Naturalist* **176**, 456–464.
- Guan, S., Southall, B. L., Vignola, J. F., Judge, J. A., and Turo, D. (2017). “Sonar inter-ping noise field characterization during cetacean behavioral response studies off Southern California,” *Acoust. Phys.* **63**, 204–215.
- Guan, S., Vignola, J., Judge, J., and Turo, D. (2015). “Airgun inter-pulse noise field during a seismic survey in an Arctic ultra shallow marine environment,” *J. Acoust. Soc. Am.* **138**, 3447–3457.
- Guerra, M., Hickmott, L., van der Hoop, J., Rayment, W., Leunissen, E., Slooten, E., and Moore, M. (2017). “Diverse foraging strategies by a marine top predator: Sperm whales exploit pelagic and demersal habitats in the Kaikōura submarine canyon,” *Deep Sea Research Part I: Oceanographic Research Papers* **128**, 98–108.
- Halfwerk, W., and Slabbekoorn, H. (2009). “A behavioural mechanism explaining noise-dependent frequency use in urban birdsong,” *Animal Behaviour* **78**, 1301–1307.
- Harris, C. M., Thomas, L., Falcone, E. A., Hildebrand, J., Houser, D., Kvadsheim, P. H., Lam, F. P. A., et al. (2018). “Marine mammals and sonar: Dose-response studies, the risk-disturbance hypothesis and the role of exposure context,” *J. Appl. Ecol.* **55**, 396–404.
- Hegna, S., Klüver, T., and Lima, J. (2018). “Benefits of continuous source and receiver side wavefields,” in *SEG Technical Program Expanded Abstracts 2018* (Society of Exploration Geophysicists, Tulsa, OK).
- Hine, J. E., Martin, R. L., and Moore, D. R. (1994). “Free-field binaural unmasking in ferrets,” *Behavioral Neuroscience* **108**(1), 196–205.
- Hines, P. C., Hicks, K., Murphy, S. M., and Taylor, N. (2015). “Measurements of signal coherence for high and low duty cycle sonars in a shallow water channel,” in *Proceedings of OCEANS 2015–Genova*, May 18–21, Genova, Italy.
- Ibsen, S. D., Au, W. W. L., Nachtigall, P. E., and Breese, M. (2009). “Functional bandwidth of an echolocating Atlantic bottlenose dolphin (*Tursiops truncatus*),” *J. Acoust. Soc. Am.* **125**, 1214–1221.
- Ibsen, S. D., Krause-Nehring, J., Nachtigall, P. E., Au, W. W. L., and Breese, M. (2011). “Similarities in echolocation strategy and click characteristics between a *Pseudorca crassidens* and a *Tursiops truncatus*,” *J. Acoust. Soc. Am.* **130**, 3085–3089.
- Isojunno, S., Curé, C., Kvadsheim, P. H., Lam, F. P. A., Tyack, P. L., Wensveen, P. J., and Miller, P. J. O. M. (2016). “Sperm whales reduce foraging effort during exposure to 1–2 kHz sonar and killer whale sounds,” *Ecol. Appl.* **26**, 77–93.
- Isojunno, S., and Miller, P. J. O. (2018). “Movement and biosonar behavior during prey encounters indicate that male sperm whales switch foraging strategy with depth,” *Front. Ecol. Evol.* **6**, 1–15.
- Isojunno, S., Wensveen, P. J., Lam, F. P. A., Kvadsheim, P. H., Von Benda-Beckmann, A. M., Martín López, L. M., Kleivane, L., Siegal, E. M., and Miller, P. J. O. (2020). “When the noise goes on: Received sound energy predicts sperm whale responses to both intermittent and continuous navy sonar,” *J. Exp. Biol.* **223**, jeb219741.
- Jensen, F. H., Johnson, M., Ladegaard, M., Wisniewska, D. M., and Madsen, P. T. (2018). “Narrow acoustic field of view drives frequency scaling in toothed whale biosonar,” *Curr. Biol.* **28**, 3878–3885.e3.
- Johnson, C. S. (1971). “Auditory masking of one pure tone by another in the bottlenosed porpoise,” *J. Acoust. Soc. Am.* **49**, 1317–1318.
- Johnson, M., Madsen, P. T., Zimmer, W. M. X., Aguilar De Soto, N., and Tyack, P. L. (2004). “Beaked whales echolocate on prey,” *Proc. R. Soc. B Biol. Sci.* **271**, 2–5.

- Jones, B. A., Stanton, T. K., Lavery, A. C., Johnson, M. P., Madsen, P. T., and Tyack, P. L. (2008). "Classification of broadband echoes from prey of a foraging Blainville's beaked whale." *J. Acoust. Soc. Am.* **123**, 1753–1762.
- Kastelein, R. A., Janssen, M., Verboom, W. C., and de Haan, D. (2005). "Receiving beam patterns in the horizontal plane of a harbor porpoise (*Phocoena phocoena*)." *J. Acoust. Soc. Am.* **118**, 1172–1179.
- Klopper, L. N., Buck, J. R., Liu, Y., and Nachtigall, P. E. (2018). "Off-axis targets maximize bearing Fisher Information in broadband active sonar." *J. Acoust. Soc. Am.* **143**, EL43–EL48.
- Klump, G. M. (1996). "Bird communication in the noisy world," in *Ecology and Evolution of Acoustic Communication in Birds* edited by D. E. Kroodsma and E. H. Miller (University Press, Ithaca, New York), pp. 321–338.
- Ladegaard, M. (2017). *Echolocation in Small Cetaceans* (Aarhus University, Aarhus, Denmark).
- Ladegaard, M., Jensen, F. H., Beedholm, K., Da Silva, V. M. F., and Madsen, P. T. (2017). "Amazon river dolphins (*Inia geoffrensis*) modify biosonar output level and directivity during prey interception in the wild." *J. Exp. Biol.* **220**, 2654–2665.
- Lam, F. P., Kvadsheim, P. H., Isojunno, S., Wenvseen, P. J., van IJsselmuide, S., Siemensma, M., Dekeling, R., and Miller, P. J. O. (2018). "Behavioural response study on the effects of continuous sonar on sperm whales in Norwegian waters—The 3S-2016-CAS cruise report," TNO report TNO2018 R10802, <http://publications.tno.nl/publication/34627070/Q3bPWP/TNO-2018-R10802.pdf> (Last viewed 4/22/2021).
- Lane, H. L., and Tranel, B. (1971). "The Lombard sign and the role of hearing in speech." *J. Hearing and Speech Research* **14**, 677–709.
- Lemons, D. W., Au, W. W. L., Vlachos, S. A., and Nachtigall, P. E. (2012). "High-frequency auditory filter shape for the Atlantic bottlenose dolphin." *J. Acoust. Soc. Am.* **132**, 1222–1228.
- Linnenschmidt, M., Beedholm, K., Wahlberg, M., Højer-Kristensen, J., and Nachtigall, P. E. (2012). "Keeping returns optimal: Gain control exerted through sensitivity adjustments in the harbour porpoise auditory system." *Proc. R. Soc. B Biol. Sci.* **279**, 2237–2245.
- Love, R. H. (1981). "A model for estimating distributions of fish school target strengths." *Deep Sea Res. Part A* **28**, 705–725.
- Madsen, P. T., Johnson, M., Aguilar De Soto, N., Zimmer, W. M. X., and Tyack, P. (2005). "Biosonar performance of foraging beaked whales (*Mesoplodon densirostris*)." *J. Exp. Biol.* **208**, 181–194.
- Madsen, P. T., and Surlykke, A. (2013). "Functional convergence in bat and toothed whale biosonars." *Physiology* **28**, 276–283.
- Madsen, P. T., Wahlberg, M., and Möhl, B. (2002). "Male sperm whale (*Physeter macrocephalus*) acoustics in a high-latitude habitat: Implications for echolocation and communication." *Behav. Ecol. Sociobiol.* **53**, 31–41.
- Madsen, P. T., Wilson, M., Johnson, M., Hanlon, R. T., Bocconcelli, A., Aguilar de Soto, N., and Tyack, P. L. (2007). "Clicking for calamari: Toothed whales can echolocate squid *Loligo pealeii*." *Aquat. Biol.* **1**, 141–150.
- Miller, P. J. O., Johnson, M. P., and Tyack, P. L. (2004). "Sperm whale behaviour indicates the use of echolocation click buzzes 'creaks' in prey capture." *Proc. R. Soc. B Biol. Sci.* **271**, 2239–2247.
- Miller, P. J. O., Kvadsheim, P., Lam, F.-P. A., Wenvseen, P. J., Antunes, R., Alves, A. C., Visser, F., Kleivane, L., Tyack, P., and Doksaeter Silve, L. (2012). "The severity of behavioral changes observed during experimental exposures of killer (*Orcinus orca*), long-finned pilot (*Globicephala melas*), and sperm whales (*Physeter macrocephalus*) to naval sonar." *Aquat. Mamm.* **38**(4), 362–401.
- Möhl, B., Wahlberg, M., Madsen, P. T., Heerfordt, A., and Lund, A. (2003). "The monopulsed nature of sperm whale clicks." *J. Acoust. Soc. Am.* **114**, 1143–1154.
- Mooney, T. A., Nachtigall, P. E., Castellote, M., Taylor, K. A., Pacini, A. F., and Esteban, J. A. (2008). "Hearing pathways and directional sensitivity of the beluga whale, *Delphinapterus leucas*." *J. Exp. Mar. Biol. Ecol.* **362**, 108–116.
- Moore, B. C. J. (2003). *An Introduction to the Psychology of Hearing* 5th ed. (Academic Press, San Diego, CA).
- Moore, P. W. B., and Pawloski, D. A. (1990). "Investigations on the control of echolocation pulses in the dolphin (*Tursiops truncatus*)," in *Sensory Abilities of Cetaceans* edited by J. A. Thomas and R. A. Kastelein (Springer, Boston), pp. 305–316.
- Nishiwaki, N., Oshumi, S., and Maeda, Y. (1963). "Changes of form in the sperm whale accompanied with growth." *Sci. Rept. Whales Res. Inst.* **17**, 1–13.
- Oliveira, C., Wahlberg, M., Johnson, M., Miller, P. J. O., and Madsen, P. T. (2013). "The function of male sperm whale slow clicks in a high latitude habitat: Communication, echolocation, or prey debilitation?." *J. Acoust. Soc. Am.* **133**, 3135–3144.
- Oscarsson-Nagel, M. D. C., Söllner, W., TrættenArmstrong, B., Nams, D., and Yeatman, P. (2019). "Marine vibrator source: Modular system with folded oscillating surface," in *Proceedings of the 81st EAGE Conference and Exhibition 2019*, Vol. 2019, pp. 1–5.
- Oxenham, A. J., and Plack, C. J. (1998). "Suppression and the upward spread of masking." *Br. J. Audiol.* **32**, 97–98.
- Planque, R., and Slabbekoorn, H. (2008). "Spectral overlap in songs and temporal avoidance in a Peruvian bird assemblage." *Ethology* **114**, 262–271.
- Popov, V. V., and Supin, A. Y. (2009). "Comparison of directional selectivity of hearing in a beluga whale and a bottlenose dolphin." *J. Acoust. Soc. Am.* **126**, 1581–1587.
- Popov, V. V., Supin, A. Y., Gvozdeva, A. P., Nechaev, D. I., Tarakanov, M. B., and Sysueva, E. V. (2020). "Spatial release from masking in a bottlenose dolphin *Tursiops truncatus*." *J. Acoust. Soc. Am.* **147**, 1719–1726.
- Porter, M., and Reiss, E. L. (1984). "A numerical method for ocean-acoustic normal modes." *J. Acoust. Soc. Am.* **76**, 244–252.
- Porter, M. B., and Buckner, H. P. (1987). "Gaussian beam tracing for computing ocean acoustic fields." *J. Acoust. Soc. Am.* **82**, 1349–1359.
- Rendell, L. E., and Whitehead, H. (2003). "Vocal clans in sperm whales (*Physeter macrocephalus*)." *Proc. R. Soc. Lond. Ser. B Biol. Sci.* **270**, 225–231.
- Rice, D. W. (1989). "Sperm whale. *Physeter macrocephalus* Linnaeus, 1775," in *Handbook of Marine Mammals* 4th ed., edited by S. H. Ridgway (Academic, London), pp. 177–233.
- Ridgway, S. H., and Carder, D. (2001). "Assessing hearing and sound production in cetacean species not available for behavioral audiograms: Experience with *Physeter*, *Kogia* and *Eschrichtius*." *Aquat. Mammals* **27**, 267–276.
- Romanenko, E. V., and Kitain, V. Y. (1992). "The functioning of the echolocation system of *Tursiops truncatus* during noise masking," in *Marine Mammal Sensory Systems* edited by J. A. Thomas, R. A. Kastelein, and A. Y. Supin (Springer, Boston), pp. 415–419.
- Saberi, K., Dostal, L., Sadralodabai, T., Bull, V., and Perrott, D. R. (1991). "Free-field release from masking." *J. Acoust. Soc. Am.* **90**(3), 1355–1370.
- Santos, M. B., Pierce, G. J., Boyle, P. R., Reid, R. J., Ross, H. M., Patterson, I. A. P., Kinze, C. C., Tougaard, S., Lick, R., Piatkowski, U., and Hernández-García, V. (1999). "Stomach contents of sperm whales *Physeter macrocephalus* stranded in the North Sea 1990–1996." *Mar. Ecol. Prog. Ser.* **183**, 281–294.
- Shaffer, J. W., Moretti, D., Jarvis, S., Tyack, P., and Johnson, M. (2013). "Effective beam pattern of the Blainville's beaked whale (*Mesoplodon densirostris*) and implications for passive acoustic monitoring." *J. Acoust. Soc. Am.* **133**, 1770–1784.
- Short, J. R. (2005). "High-frequency ambient noise and its impact on underwater tracking ranges." *IEEE J. Ocean. Eng.* **30**, 267–274.
- Sills, J. M., Southall, B. L., and Reichmuth, C. (2017). "The influence of temporally varying noise from seismic air guns on the detection of underwater sounds by seals." *J. Acoust. Soc. Am.* **141**, 996–1008.
- Simmons, J. A. (2017). "Noise interference with echo delay discrimination in bat biosonar." *J. Acoust. Soc. Am.* **142**, 2942–2952.
- Sivle, L. D., Kvadsheim, P. H., Curé, C., Isojunno, S., Wenvseen, P. J., Lam, F. P. A., Visser, F., Kleivane, L., Tyack, P. L., Harris, C. M., and Miller, P. J. O. (2015). "Severity of expert-identified behavioural responses of humpback whale, minke whale, and northern bottlenose whale to naval sonar." *Aquat. Mamm.* **41**, 469–502.
- Slabbekoorn, H., Dooling, R. J., Popper, A. N., and Fay, R. R. (2018). "Communication Masking by Man-Made Noise," in *Effects of Anthropogenic Noise on Animals* edited by H. Slabbekoorn, R. J. Dooling, A. N. Popper, and R. R. Fay (Springer, New York), pp. 23–46.
- Smith, P. F. (1954). "Further measurements of the sound scattering properties of several marine organisms." *Deep Sea Res.* **2**, 71–79.
- Southall, B. L., Bowles, A. E., Ellison, W. T., Finneran, J. J., Gentry, R. L., Greene, C. R., Jr., Kastak, D., Ketten, D. R., Miller, J. H., Nachtigall, P.

- E., Richardson, W. J., Thomas, J. A., and Tyack, P. L. (2007). "Marine mammal noise exposure criteria: Initial scientific recommendations," *Aquat. Mamm.* **33**(4), 411–509.
- Sümer, S., Denzinger, A., and Schnitzler, H. U. (2009). "Spatial unmasking in the echolocating Big Brown Bat, *Eptesicus fuscus*," *J. Comp. Physiol. A* **195**, 463–472.
- Teloni, V., Mark, J. P., Patrick, M. J. O., and Peter, M. T. (2008). "Shallow food for deep divers: Dynamic foraging behavior of male sperm whales in a high latitude habitat," *J. Exp. Mar. Biol. Ecol.* **354**, 119–131.
- Thomas, J. A., and Turl, C. W. (1990). "Echolocation characteristics and range detection threshold of a false killer whale (*Pseudorca crassidens*)," in *Sensory Abilities of Cetaceans* (Springer, New York), pp. 321–334.
- Tønnesen, P. (2020). "Echolocation of deep-diving toothed whales," Ph.D. Dissertation, Department of Biology, Aarhus University, Denmark.
- Tønnesen, P., Oliveira, C., Johnson, M., and Madsen, P. T. (2020). "The long-range echo scene of the sperm whale biosonar," *Biology Letters* **16**, 8, 20200134.
- Trickey, J. S., Branstetter, B. K., and Finneran, J. J. (2010). "Auditory masking of a 10 kHz tone with environmental, comodulated, and Gaussian noise in bottlenose dolphins (*Tursiops truncatus*)," *J. Acoust. Soc. Am.* **128**, 3799–3804.
- Turl, C. W., Penner, R. H., and Au, W. W. L. (1987). "Comparison of target detection capabilities of the beluga and bottlenose dolphin," *J. Acoust. Soc. Am.* **82**, 1487–1491.
- van Vossen, R., Beerens, S. P., and van der Spek, I. E. (2011). "Anti-submarine warfare with continuously active sonar," *Sea Technol. Mag.* 33–35.
- Verfuß, U. K., Miller, L. A., and Schnitzler, H. U. (2005). "Spatial orientation in echolocating harbour porpoises (*Phocoena phocoena*)," *J. Exp. Biol.* **208**, 3385–3394.
- Verzijden, M. N., Ripmeester, E. A. P., Ohms, V. R., Snelderwaard, P., and Slabbekoorn, H. (2010). "Immediate spectral flexibility in singing chiffchaffs during experimental exposure to highway noise," *J. Experimental Biology* **213**(15), 2575–2581.
- Vliegen, J., and Oxenham, A. J. (1999). "Sequential stream segregation in the absence of spectral cues," *J. Acoustical Society America* **105**(1), 339–346.
- von Benda-Beckmann, A. M., Thomas, L., Tyack, P. L., and Ainslie, M. A. (2018). "Modelling the broadband propagation of marine mammal echolocation clicks for click-based population density estimates," *J. Acoust. Soc. Am.* **143**, 954–967.
- Wartzok, D., and Ketten, D. R. (1999). "Marine mammal sensory systems," in *Biology of Marine Mammals* edited by J. E. Reynolds and S. Rommel (Smithsonian Institution Press, Washington, DC), pp. 117–175.
- Watkins, W. A., and Schevill, W. E. (1977). "Sperm whale codas," *J. Acoust. Soc. Am.* **62**, 1485–1490.
- Watwood, S. L., Miller, Patrick J. O., Johnson, M., Madsen, P. T., and Tyack, P. L. (2006). "Deep-diving foraging behaviour of sperm whales (*Physeter macrocephalus*)," *J. of Animal Ecology* **75**, 814–825.
- Wenz, G. M. (1962). "Acoustic ambient noise in the ocean: Spectra and sources," *J. Acoust. Soc. Am.* **34**, 1936–1956.
- Weston, D. E. (1971). "Intensity-range relations in oceanographic acoustics," *J. of Sound and Vibration* **18**(2), 271–287.
- Whitehead, H. (2003). *Sperm Whales: Social Evolution in the Ocean* (University of Chicago, Chicago).
- Whitehead, H. (2018). "Sperm whale: *Physeter macrocephalus*," in *Encyclopedia of Marine Mammals* 3rd ed., edited by B. Würsig, J. G. M. Thewissen, and K. M. Kovacs (Academic, London), pp. 919–925.
- Wiley, R. H., and Richards, D. G. (1982). "Adaptations for acoustic communication in birds: Sound transmission and signal detection," in *Acoustic Communication in Birds* edited by D. E. Kroodsma & E. H. Miller (Academic Press, New York). Vol. 1, pp. 131–181.
- Wisniewska, D. M., Johnson, M., Teilmann, J., Rojano-Doñate, L., Shearer, J., Sveegaard, S., Miller, L. A., Siebert, U., and Madsen, P. T. (2016). "Ultra-high foraging rates of harbor porpoises make them vulnerable to anthropogenic disturbance," *Curr. Biol.* **26**, 1441–1446.
- Wisniewska, D. M., Ratcliffe, J. M., Beedholm, K., Christensen, C. B., Johnson, M., Koblitz, J. C., Wahlberg, M., and Madsen, P. T. (2015). "Range-dependent flexibility in the acoustic field of view of echolocating porpoises (*Phocoena phocoena*)," *Elife* **4**, e05651.
- Ya Supin, A., and Nachtigall, P. E. (2013). "Gain control in the sonar of odontocetes," *J. Comp. Physiol. A* **199**, 471–478.
- Zimmer, W. M. X., Tyack, P. L., Johnson, M. P., and Madsen, P. T. (2005). "Three-dimensional beam pattern of regular sperm whale clicks confirms bent-horn hypothesis," *J. Acoust. Soc. Am.* **117**, 1473–1485.